UNIVERSITY OF VERONA

DEPARTMENT OF

Diagnostics and Public Health

DOCTORAL PROGRAM IN

Applied Life and Health Sciences

WITH THE FINANCIAL CONTRIBUTION OF

University of Verona

XXXVIII Cycle / 2022-2025

ANTIOXIDANT STRATEGIES FOR CELLULAR AGING: THE ROLE OF HOMOTAURINE AND GLUTATHIONE

S.S.D. BIOS-08/A

Coordinator: Prof./ssa Simone Accordini

Signature _____

Supervisor: Prof./ssa Maria Teresa Valenti

Signature _____

Co-Supervisor: Prof./ssa Luca Dalle Carbonare

Signature _____

Doctoral Student: Dott./ssa Francesca Cristiana Piritore

Signature _____

This work is licensed under a Creative Commons Attribution-NonCommercial-NoDerivative 4.0 International. To read a copy of the license, visit the web page:

https://creativecommons.org/licenses/by-nc-nd/4.0/

Attribution -You must give appropriate credit, provide a link to the license, and indicate if changes were made. You may do so in any reasonable manner, but not in any way that suggests the licensor endorses you or your use.

Noncommercial- You may not use the material for commercial purposes.

No Derivatives- If you remix, transform, or build upon the material, you may not distribute the modified material.

Antioxidant strategies for cellular aging: the role of homotaurine and glutathione

Francesca Cristiana Piritore

Verona, December 2025.

CONTENTS

ABBREVIATIONS

- **Ab I:** primary antibody
- **Ab II:** secondary antibody
- **AD:** Alzheimer's disease
- **BBB:** blood–brain barrier
- **CCK-8:** Cell Counting Kit-8
- **CTRL:** control
- **DCFDA:** 2',7'-dichlorofluorescein diacetate
- **DiI:** 1,1′-dioctadecyl-3,3,3′,3′-tetramethylindocarbocyanine perchlorate
- **DiO**: 3,3′-dioctadecyloxacarbocyanine perchlorates
- **Dpf:** days post-fertilization
- **DSBs:** DNA double-strand breaks
- **EVs:** extracellular vesicles
- **GABA:** γ-Aminobutyric acid
- **GC:** Wild type
- **GFAP:** Glial fibrillary acidic protein
- **GFP:** green fluorescence protein
- **GPx:** glutathione peroxidase
- **GR:** glutathione reductase
- **GSH:** glutathione
- **GSSG:** oxidized glutathione
- **H_2O_2:** hydrogen peroxide
- **iPSC:** human-induced pluripotent stem cells
- **JNK:** c-Jun N-terminal kinase
- **KDRL:** kinase insert domain receptor
- **LC3B:** Microtubule-associated protein 1A/1B-light chain 3B
- **LRRK2:** leucine-rich repeat kinase 2
- **MAP2:** Microtubule-associated protein 2
- **MFI:** median fluorescence intensity
- **MSCs:** Human mesenchymal stem cells
- **mtDNA:** mitochondrial DNA

- **MUT:** mutated
- **NAFLD:** non-alcoholic fatty liver disease
- **NESCs:** Neuronal epithelial stem cells
- **NTA:** Nanoparticle tracking analysis
- **SASP:** senescence-associated secretory phenotype
- **OA:** osteoarthritis
- **OS:** oxidative stress
- **PD:** Parkinson's disease
- **PFA:** paraformaldehyde
- **PI:** propidium iodide
- **PVDF:** polyvinylidene difluoride
- **ROS:** reactive oxygen species
- **RT-qPCR:** Real-time quantitative PCR
- **RT:** room temperature
- **RUNX 2:** Runt-related transcription factor 2
- **SA-β-gal:** senescence-associated β-galactosidase
- **SD:** Standard deviation
- **SESN 1:** Sestrin 1
- **SESN 2:** Sestrin 2
- **SH-SY5Y**: Human neuroblastoma cells
- **SOD:** superoxide dismutases
- **TBHP:** *tert*-Butyl hydroperoxide
- **TEM:** Transmission electron microscopy
- **TH:** Tyrosine hydroxylase
- **VEGFR2:** vascular endothelial growth factor receptor 2

ABSTRACT

Aging and cellular senescence are two closely interconnected processes. Senescence is characterized by a permanent cell-cycle arrest in response to stress conditions, with the aim of preserving the integrity of the organism. However, the accumulation of senescent cells within tissues contributes to the acceleration of the aging process and to the possible onset of associated pathologies, including neurodegenerative diseases. Among the main factors that induce senescence, oxidative stress plays a crucial role, as it results from an imbalance between the production of reactive oxygen species (ROS) and the ability of the antioxidant system to neutralize them.

The aim of this study was to investigate the potential of homotaurine, a small molecule with neuroprotective properties, and glutathione (GSH), an intracellular antioxidant, as protective agents on mesenchymal stem cells and neuronal models such as Parkinson's disease organoids or neuroblastoma cells. Homotaurine exhibited strong protective activity, enhancing cell viability and reducing oxidative stress through the modulation of key stress-related pathways. In *in vivo* models, it was shown to promote angiogenesis and osteogenesis. Moreover, in organoids Parkinson's disease models, treatment induced significant neuroprotective effects, including increased β-catenin levels and reduced ROS levels. GSH was used to treat Mesenchymal Stem Cells (MSCs) and SH-SY5Y neuroblastoma cells. GSH was administered both directly and via extracellular vesicles (EVs) derived from GSH-pretreated MSCs. In this case as well, the data revealed a marked antioxidant capacity, with clear improvements in cell viability and a reduction in oxidative-stress markers. The EVs from pretreated MSCs retained the effects of GSH, suggesting an effective and biocompatible delivery approach.

Overall, the results of this study confirm that homotaurine and glutathione can modulate key processes involved in senescence and aging, opening new perspectives for targeted interventions aimed at the prevention and treatment of neurodegenerative diseases.

ABSTRACT (ITALIANO)

L’invecchiamento e la senescenza cellulare rappresentano due processi strettamente interconnessi. La senescenza, infatti, è caratterizzata da un blocco permanente del ciclo cellulare che viene attuato in risposta a condizioni di stress con lo scopo di preservare l’integrità dell’organismo. Tuttavia, un accumulo di cellule senescenti nei tessuti contribuisce all’accelerazione del processo di invecchiamento e alla possibile insorgenza di patologie ad esso associate, tra cui le malattie neurodegenerative. Tra i principali fattori che inducono la senescenza, lo stress ossidativo riveste un ruolo cruciale, poiché deriva da un disequilibrio tra la produzione di specie reattive dell’ossigeno e la capacità del sistema antiossidante di neutralizzarle.

L'obiettivo di questo studio è stato quello di indagare le potenzialità dell’omotaurina, una piccola molecola con proprietà neuroprotettive, e del glutatione, un antiossidante intracellulare, come agenti protettivi su cellule mesenchimali e modelli neuronali come organoidi di Parkinson o cellule di neuroblastoma. L’omotaurina ha mostrato un’elevata attività protettiva, migliorando la vitalità cellulare e riducendo lo stress ossidativo tramite la modulazione dei principali pathway coinvolti allo stress. Nei modelli in vivo ha dimostrato di promuovere l’angiogenesi e l’osteogenesi. Inoltre, nei modelli 3D di malattia di Parkinson, il trattamento ha dimostrato significativi effetti neuroprotettivi, con un aumento dei livelli di β-catenine riducendo i livelli dei ROS. Il GSH è stato utilizzato per il trattamento di MSCs e SH-SY5Y, a quest’ultime è stato somministrato sia direttamente sia tramite EVs da MSCs pretrattate con GSH. Anche in questo caso, i dati hanno mostrato una marcata capacità antiossidante, con evidente miglioramento della vitalità cellulare e riduzione dei marcatori dello stress ossidativo. Le vescicole delle MSCs pretrattate hanno mantenuto l’effetto del GSH, indicando un approccio veicolare potenzialmente efficace e biocompatibile. Nel complesso, i risultati di questo studio confermano che omotaurina e glutatione possono modulare i processi chiave di senescenza e invecchiamento, aprendo nuove prospettive per interventi mirati alla prevenzione e al trattamento di patologie neurodegenerative.

1. INTRODUCTION

1.1 From stress to arrest: mechanisms of cellular senescence

Cellular senescence is a condition in which cells cease to divide indefinitely and experience profound alterations in their properties and capabilities (Petrova et al., 2016). It is characterized by an almost irreversible growth arrest in response to a range of stressors, such as telomere shortening, oncogene activation, DNA damage, oxidative stress and secretion of the senescence-associated secretory phenotype (SASP). Cellular senescence was first described by Leonard Hayflick and Paul Moorhead in 1961 using diploid fibroblast cell lines that ceased to divide after 40–60 population doublings (Zhang et al., 2022).This kind of senescence, known as replicative senescence, depends on telomeres gradually getting shorter. Other forms of cellular senescence can occur prematurely and resemble replicative senescence, although they are not linked to telomere shortening. Sub cytotoxic stimuli such as UV, γ-irradiation, H_2O_2 and hyperoxia can cause oncogene activation, DNA damage and oxidative stress that leads to senescence in a variety of proliferative cell types (Figure 1) (Petrova et al., 2016; K. Wang et al., 2024). Senescent cells undergo morphological changes, accumulating stress granules, flattening, and vacuolizing (Sharpless & Sherr, 2015).

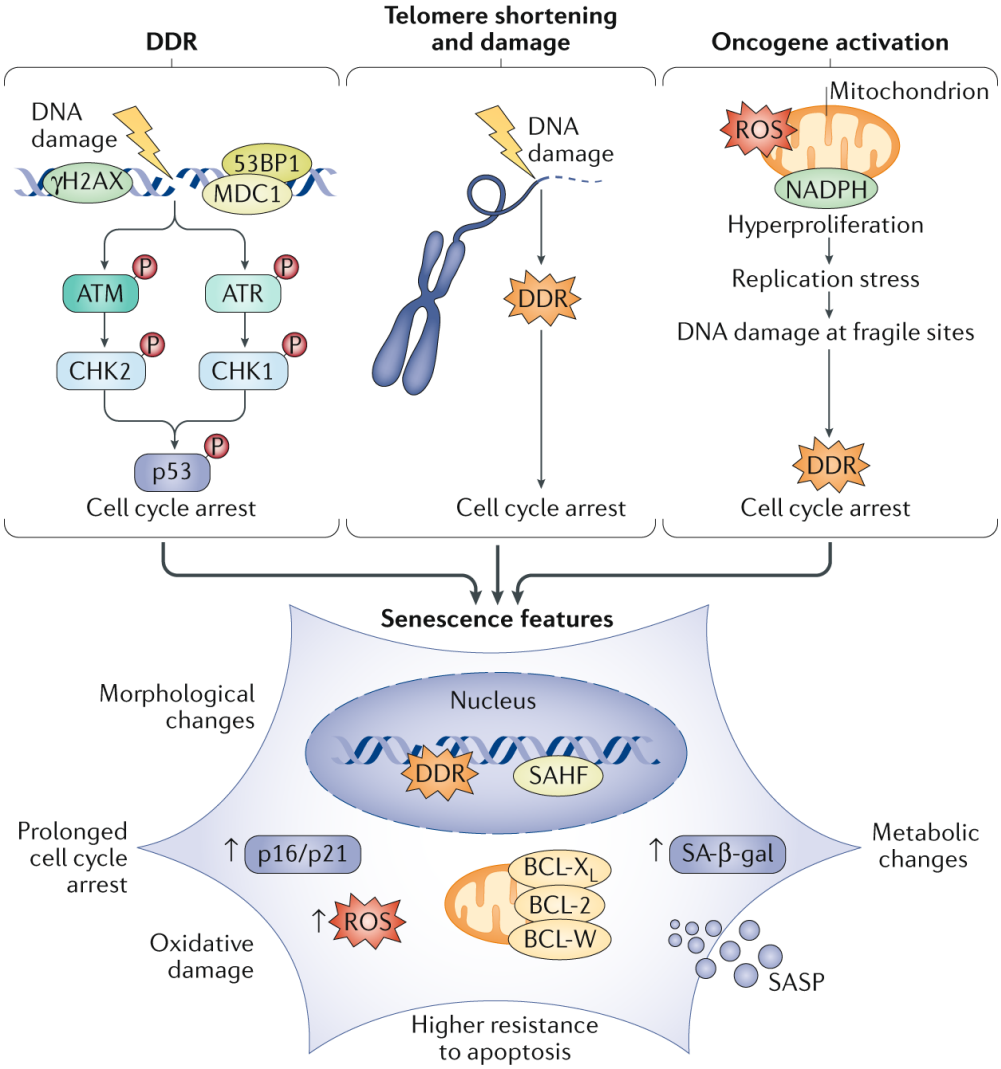

***Figure 1: Causes of senescence and its effect on* cells**. Cellular senescence can be induced by several stress signals, such as the DNA damage response (DDR), telomere shortening and oncogene activation. These pathways lead to cell cycle arrest through signaling cascades involving ATM/ATR, CHK1/CHK2 and p53. Senescent cells are characterized by morphological and metabolic changes, like persistent DDR signaling, an upregulation of cell cycle inhibitors, accumulation of ROS, resistance to apoptosis and the presence of the senescence-associated secretory phenotype (SASP). (Di Micco et al., 2021).

Furthermore, the expression of cyclin-dependent kinase inhibitors like p16 and p21, the activation of the p53/Rb pathway and the secretion of the SASP are characteristics of the senescent phenotype. Cells enter a senescent state when p53 is upregulated. The tumor suppressor protein, p53 (encoded by TP53) is widely recognized as the master regulator of the cellular stress response (Farnebo et al., 2010). When DNA is damaged, checkpoint proteins like p53 are expressed, which triggers the activation of sensor kinases (ATM, ATR, and DNA-dependent protein kinase) and results in the up-regulation of p21 (Pezone et al., 2023). p21 mainly acts as a temporary cell cycle inhibitor, which creates a crucial window of opportunity for DNA damage repair prior to the cell cycle's subsequent progression. Therefore, p21-induced senescence is often reversible (Goyal et al., 2025). On the other

hand, if this p21-induced arrest continues, p16 is produced. In contrast to p21, p16 permanently stops cell division by causing an irreversible halt in the cell cycle. Moreover, other factors can also directly activate p16. According to a study by Lyons et al., stressed mice exhibited more senescent cells overall, with p16 levels being particularly high (Lyons et al., 2025). This illustrates how stress can impede the aging process. Furthermore, SASP, which includes growth factors, matrix remodeling enzymes and pro-inflammatory cytokines, can have both autocrine and paracrine effects, promoting senescence and changing the tissue microenvironment. Senescent cells can proliferate due to lifestyle choices and environmental factors. According to a recent study, nanoplastics can be absorbed by cells and cause increased levels of reactive oxygen species (ROS), senescence-associated β-galactosidase (SA-β-gal) and γH2AX, a hallmark of DNA damage (Wang et al., 2024). Oxidative stress plays an important role in cellular senescence. There exists a relationship between p16 and ROS accumulation; in fact, p16 downregulation results in an increase in ROS levels (Wagner et al., 2024). The quantity of ROS in cells is meticulously regulated. When this equilibrium is upset, an excess of ROS can accumulate, which can cause cellular senescence and accelerate aging (Guo et al., 2020). In post-mitotic somatic cells, elevated ROS levels can damage various cell components and trigger certain signaling cascades (Chen et al., 2015). Specifically, ROS positively influence senescence through the ASK1/JNK/p38 signaling pathway. Normally, a complex with reduced TRX (thioredoxin) keeps ASK-1 (apoptosis signal-regulated kinase-1) inactive. However, under extreme stress, certain cysteine residues on TRX are oxidized by hydrogen peroxide (H_2O_2). Because of this oxidation, ASK-1 dissociates and becomes active, which in turn activates p38 and JNK (c-Jun N-terminal kinase) (Kirtonia et al., 2020). p38 is known to induce p53, which causes cells to enter a senescence state (Han et al., 2020). Mitochondria are essential for preserving cell homeostasis since they are the main source of cellular ATP and reactive oxygen species (ROS). In a study by Noh et al., the GRSF1, a part of mitochondrial RNA granules, was found to be a crucial protein in preserving mitochondrial function. Numerous senescence traits, including growth stop, oxidative stress, DNA damage, and senescence-associated secretory phenotype (SASP), were connected to mitochondrial stress brought on by the loss of this enzyme (Noh et al., 2018). These cellular mechanisms are directly linked to organismal aging.

1.2 Aging: its hallmarks and their systemic impact

Age is a major risk factor for many chronic diseases, including as cancer, osteoporosis, diabetes, neurological diseases and heat-related ailments. In societies with an aging population, neurodegenerative diseases represent one of the major public health concerns. These are chronic conditions that usually manifest as a slow but unrelenting loss of neurons and synaptic connections, which eventually results in deficits in cognition, motor function, and behavior (Pandey, 2025). Alzheimer's disease (AD) is the most common type and the main contributor to dementia in the elderly (Association, 2019). The buildup of β-amyloid plaques and neurofibrillary tangles made of hyperphosphorylated tau is a hallmark of AD, which causes cortical degeneration and gradual cognitive loss (Sajjad et al., 2018). Parkinson's disease (PD) is the second most common neurodegenerative disorder, primarily associated with the loss of dopaminergic neurons in the substantia nigra. Clinically, it manifests with bradykinesia, rigidity and resting tremor, often accompanied by a wide range of non-motor symptoms (Sharma et al., 2025). Huntington's disease is an autosomal dominant genetic disorder that typically manifests in adulthood, presenting cognitive and psychiatric alterations along with choreic motor symptoms. (Jesuthasan et al., 2025). Reduced bone mass and microarchitectural degradation are hallmarks of osteoporosis, which makes bones more brittle and prone to fractures. Importantly, bone loss is a result of aging-related hormonal changes, specifically postmenopausal estrogen insufficiency, as well as compromised calcium and vitamin D metabolism (Gildee C, 2025). Osteoporotic fractures, especially of the hip and spine, are a significant cause of disability, loss of independence and mortality in the elderly population (Selçuk, 2025).

Understanding the underlying mechanisms of aging is crucial to developing effective therapeutic strategies because these conditions are closely linked to the biological aging process (Pandey, 2025). The complexity of aging has been explained by a variety of ideas throughout the years, but none have adequately identified the specific biological processes that underlie it. An important breakthrough came in 2023 when López-Otín et al. defined twelve characteristics that were divided into three groups, broadening the conceptual framework of aging (Figure 2) (López-Otín et al., 2023).

Figure 2: The characteristics of aging. Aging is characterized by several biological processes which contribute to the progressive decline in physiological function over time *(López-Otín et al., 2023).*

These include: integrative effects, such as stem cell exhaustion, chronic inflammation and impaired intercellular communication; antagonistic reactions, such as mitochondrial dysfunction and cellular senescence; and primary drivers, such as DNA damage and telomere shortening (López-Otín et al., 2023). Crucially, these characteristics are linked by feedback processes that gradually quicken physiological deterioration rather than functioning separately (López-Otín et al., 2023). Numerous organ systems gradually lose their integrity and functionality as aging results in complex physiological changes. Sometimes this degeneration happens faster than anticipated; this is referred to as accelerated aging. This disorder increases the likelihood of comorbidities, chronic diseases and even early mortality (Andonian et al., 2024; Ragnoli et al., 2025). Aging is thought to be caused

naturally by the buildup of DNA damage, which is driven by the attack of endogenous and external genotoxins (da Silva & Schumacher, 2021). Neurological symptoms and early aging are closely linked to mutations in DNA repair genes and abnormalities in DNA repair pathways in both human and animal models. It has been noted that a number of neurodegenerative illnesses, including Alzheimer's disease (AD), have compromised DNA damage repair, namely the repair of DNA double-strand breaks (DSBs) (Nieto-Estevez et al., 2022). Impaired cellular respiration and increased oxidative stress are hallmarks of mitochondrial dysfunction, and they both work together to induce cellular senescence. For example, Song et al. showed that in dermal fibroblasts, a lack of Carnitine Acetyltransferase (CRAT), an enzyme mainly found in the mitochondrial matrix that facilitates the reversible transfer of acetyl groups between acetyl-CoA and acetylcarnitine, impairs mitochondrial metabolism, encourages the buildup of ROS and triggers the cGAS–STING pathway through the release of cytosolic mitochondrial DNA (mtDNA), which ultimately results in cellular senescence (Song et al., 2023). The term "inflammaging" refers to the continuous low-grade inflammation that SASP contributes to (Lawrence et al., 2024).

Independent of acute immune activation, a persistent, low-grade pro-inflammatory state progressively damages tissues and organs, exacerbating age-associated functional decline and increasing susceptibility to disease (Ferrucci & Fabbri, 2018).

Senescence is not only a cellular response to stress but also a driving force of organismal aging, linking molecular dysfunction to multi-organ deterioration. This highlights the importance of investigating the molecular mechanisms, with the goal of creating therapeutic strategies to extend lifespan and mitigating chronic age-relate diseases.

1.3 Cellular Defense against oxidative stress

Reactive oxygen species (ROS) are produced naturally as a product of aerobic metabolism in cells. They are chemically reactive molecules containing oxygen, such as superoxide anions, hydrogen peroxide and hydroxyl radicals (Juan et al., 2021).

Their production is a fundamental and beneficial phenomenon for the healthy operation, defense and survival of cells within physiological bounds.

At controlled levels, ROS act as signaling molecules, regulating processes such as gene expression, apoptosis and immune response (Averill-Bates, 2024). Nevertheless, an imbalance in ROS production and neutralization could result in the buildup of harmful ROS intermediate products, which could cause oxidative stress (OS), a condition that damages

lipids, proteins and DNA (Figure 3). Long-term elevated OS has been implicated in a few potentially fatal pathological illnesses, including cancer, heart disease, diabetes, autoimmune diseases, neurological problems and aging (Hajam et al., 2022).

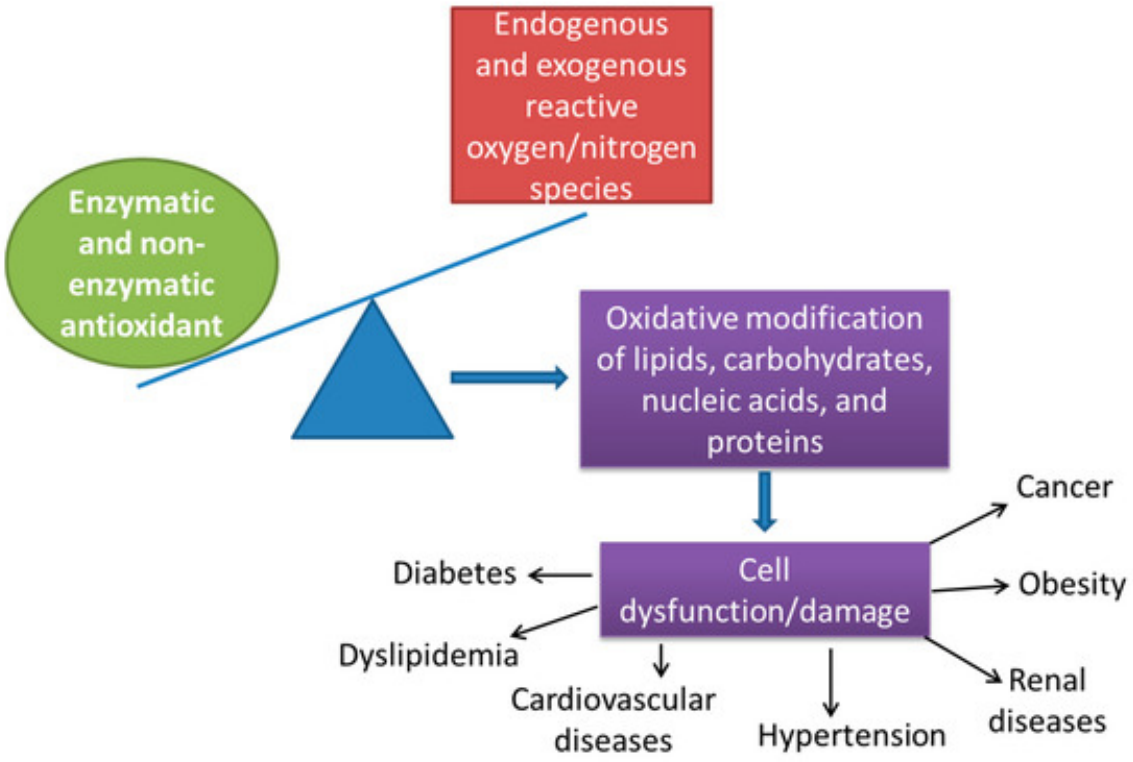

Figure 3: Impact of Oxidative Stress. An imbalance between reactive oxygen species (ROS) and antioxidant defenses leads to oxidative stress, resulting in cellular damage that contribute to the development of various diseases *(Pellegrino et al., 2019).*

Cells maintain redox homeostasis by scavenging ROS through both endogenous and exogenous antioxidant systems which neutralize ROS effects (Zhu et al., 2023).

The term "antioxidant" describes a broad class of molecules (bioactive substances and enzymatic complexes) that, when found in trace amounts (micronutrients) in the body, can shield organic substrates—both synthetic (plastics, oils) and natural (phospholipids, proteins, and DNA)—from the damaging effects of free radicals. Since they prevent the creation of the so-called initiator radicals, all antioxidants that limit or reduce the generation of radicals are recognized as preventive agents (Varesi et al., 2022). Endogenous antioxidants, including glutathione (GSH), peroxiredoxins, catalases and superoxide dismutases (SOD), are crucial in halting oxidative damage brought on by both internal and external factors (Giordano et al., 2014). Is known that oxidative stress and autophagy are

functionally linked (Li et al., 2015). Notably, autophagy acts as a critical intracellular antioxidant pathway, removing damaged organelles and oxidized macromolecules, thus preserving cellular integrity, particularly in neurons (Ornatowski et al., 2020). LC3B and p62 are two of the key proteins involved in the autophagy process. In particular, LC3B (microtubule-associated protein 1A/1B-light chain 3B) plays a fundamental role in autophagosome formation: the change from LC3B-I to LC3B-II is a typical sign of autophagosome membrane recruitment and growth (Chen et al., 2025). p62 (also known as SQSTM1) is another significant protein which acts as a selective autophagy receptor. It interacts with LC3B through its LIR motif, binds ubiquinated cargo via its UBA domain and transports aggregated or damaged proteins to the autophagosome for degradation. Because p62 itself is degraded via autophagy, its levels decrease when autophagy is active (Liu et al., 2016). The main exogenous antioxidants, also known as diet-derived antioxidants, are vitamin C, vitamin E, vitamin B6, retinol and β-carotene complement endogenous defenses by neutralizing ROS from environmental sources and supporting overall cellular balance (Pruteanu et al., 2023; Zhu et al., 2023). The interplay between endogenous and exogenous antioxidant is therefore crucial in preventing oxidative stress-related cellular disfunction, aging and disease progression (Jena et al., 2023). In this context, particular attention should be given to GSH, the most abundant endogenous antioxidant found in cells (Zhang & Forman, 2012).

1.4 Glutathione: A Central Regulator of Redox Homeostasis and Terapeutic Target

The natural tripeptide glutathione, which is γ-l-glutamyl-l-cysteinylglycine, plays a crucial part in maintaining redox equilibrium. Reduced GSH and oxidized glutathione (GSSG) are the two forms of glutathione that are produced by the enzymatic activity of glutathione reductase (GR), which catalyzes the reduction of one GSSG into two GSH at the expense of NADPH and glutathione peroxidase (GPx), which forms a disulphide bond between two GSH in one GSSG (Varesi et al., 2022). It is essential for lowering oxidative stress, preserving redox equilibrium, improving metabolic detoxification and controlling the immunological system. Low or inadequate GSH levels have been linked to several chronic, age-related illnesses, including those involving neurodegeneration, mitochondrial malfunction and even cancer (Minich & Brown, 2019).

Due to its essential function in cellular defense and redox balance, GSH is a crucial molecular target in aging and degenerative diseases.

It is well established that GSH levels decline with age. Numerous clinical illnesses, including diabetes, cancer, arthritis, cardiovascular, neurodegenerative diseases and others, are linked to low levels of GSH (Kalamkar et al., 2022). In several pathological disorders, exogenous GSH injection has shown promise as a therapeutic strategy to combat oxidative stress and restore redox balance (Allen & Bradley, 2011).

A recent clinical trial showed that daily oral supplementation of GSH was effective in raising GSH levels in oral buccal cells and various intra- and extra-cellular blood compartments. Research in laboratory animals has shown that oral GSH is bioavailable and effective at enhancing blood and tissue GSH levels and can protect against aging-related impairments in immune function, influenza infections and cancer. GSH enhancement is a potentially significant approach in the treatment and prevention of disorders associated with GSH-depletion. Studies linking dietary GSH intake with increased blood levels and a lower risk for cancer support the use of GSH administered orally (Sinha et al., 2018). For example, GSH supplementation has been linked to neuroprotective effects in ischemic stroke models (Wang et al., 2022) and enhanced insulin sensitivity in patients with type 2 diabetes (Madathil et al., 2023). Exogenous GSH has demonstrated encouraging results as a treatment for a number of illnesses, including infections like HIV and COVID-19 (Guloyan et al., 2020), non-alcoholic fatty liver disease (NAFLD) and neurological diseases like Parkinson's disease (Santacroce et al., 2023). However, GSH is quickly degraded in the bloodstream and the blood–brain barrier (BBB) severely impairs its ability to reach the central nervous system (Li et al., 2021), particularly for oral formulations. Current research is looking into new delivery methods such liposomal or nanoparticle-encapsulated GSH to improve cellular uptake (Ahmad et al., 2021; Guloyan et al., 2020).

Exogenous GSH's therapeutic potential is still gaining attraction in disciplines like neurology, endocrinology and gerontology, despite these drawbacks, confirming its usefulness as an adjuvant in the treatment of illnesses linked to oxidative stress.

Continued advancements in delivery technologies are expected to further strengthen its role as an adjuvant treatment for diseases characterized by oxidative stress and redox imbalance. Given these considerations, the importance of tightly controlled redox mechanisms becomes particularly evident in the field of regenerative medicine, where mesenchymal stem cells (MSCs) rely heavily on balanced oxidative conditions to preserve their viability, differentiation capacity and therapeutic potential.

1.5 Therapeutic Potential of Homotaurine Across Neurodegeneration and Regenerative Medicine

Homotaurine, also known as tramiprosate, was initially discovered in various types of sea red algae (Caltagirone et al., 2012). It is a permeable substance that can cross the blood-brain barrier and prevent Aβ (β-amyloid peptides) aggregation and deposition by preventing Aβ misfolding, oligomer formation and elongation (Toppi et al., 2022). Its possible neuroprotective qualities have drawn attention to it. It was initially explored in the context of Alzheimer's disease because of its potential to prevent the accumulation of Aβ, one of the hallmarks of this degenerative condition (Minoia et al., 2025). Homotaurine slows brain atrophy and improves cognitive impairment in people with mild to severe AD by lowering Aβ levels in their cerebrospinal fluid (Bossù et al., 2018). Additionally, homotaurine is an analog of GABA (γ-Aminobutyric acid), an inhibitory neurotransmitter that plays a key role in promoting anti-inflammatory characteristics in glial function. Accordingly, recent research has suggested homotaurine as a potential treatment for inflammatory and autoimmune conditions, such as multiple sclerosis (Tian et al., 2018).

According to a study by Toppi et al., administering homotaurine to patients with mild cognitive impairment resulted in a decrease in the pro-inflammatory cytokine IL-18 and an increase in the anti-inflammatory cytokines IL-33 and IL-10, demonstrating the strong anti-inflammatory effect of this treatment (Toppi et al., 2022). Moreover, homotaurine may preserve retinal cells, which would support its prospective use outside of the central nervous system (Davinelli et al., 2017). It has been demonstrated that homotaurine lowers ROS levels, improves cell viability and stimulates angiogenesis and osteogenesis. Additionally, it enhances Wnt/β-catenin signaling and reduces oxidative stress in models of Parkinson's disease, confirming its potential as a multipurpose protective agent (Minoia et al., 2025). These results demonstrate homotaurine's potential as a bioactive chemical for neurodegenerative diseases as well as more general regenerative and anti-inflammatory treatment approaches.

1.6 Biology of Mesenchymal Stem Cells and Their Therapeutic Mechanisms

The study done in the 1960s by Friedenstein, who observed that bone marrow is a source of stem cells for mesenchymal tissue, is the foundation for our knowledge of mesenchymal stem cells (MSCs) (Qin et al., 2014). He found that these cells resemble fibroblasts and are plastic-adherent, with the ability to develop into chondrocytes, adipocytes and osteoblasts (Qin et al., 2014). MSC-like populations have been extracted from autologous and allogeneic sources, such as muscle, adipose tissue, lung, synovial fluids, periodontal ligament, peripheral blood and marrow spaces of long bones, even though MSCs were first discovered in bone marrow. MSCs can also be extracted from dental pulp, the placenta and the blood of the umbilical cord (Samsonraj et al., 2017). However, as MSCs from diverse origins have varying capacities to develop into distinct cell lineages, it is crucial to determine their source (Qin et al., 2014). There is yet no distinct transcription factor that is exclusive to MSCs (Gayatri Jayendran Nair et al., 2023), for this reason in 2006, the International Society of Cellular Therapy characterized MSCs using the following three criteria in order to properly characterize them:

- Under normal tissue culture conditions, MSCs must attach to plastic;
- MSCs must display specific cell surface markers such CD73, CD90, and CD105; they do not express HLA-DR surface molecules, CD45, CD34, CD14, or CD11b, CD79, or CD19;
- *In vitro*, MSCs must be able to develop into adipocytes, chondroblasts and osteoblasts (S. Wang et al., 2012).

MSCs show notable variability based on their tissue of origin, with different chromatin accessibility profiles and gene expression patterns, according to transcriptional and epigenetic investigations. Notably, resident MSC populations can vary greatly, even within a single tissue, with several subpopulations with distinct traits. Despite this variation, mounting data indicates that MSCs grown *in vitro* and in situ are both able to actively modulate local immune responses and detect pathophysiological changes in their surroundings (Rivera-Cruz et al., 2017). MSCs support tissue regeneration and repair as well as homeostasis maintenance through their dynamic interaction with the tissue immune niche (Wang et al., 2022). Self-renewal and the capacity to develop into several cell lineages are two of the stem cells' encouraging traits. As a result, they have been thoroughly studied for potential therapeutic uses in a range of human illnesses, including cancer, spinal cord

injuries, neurodegenerative diseases (including Parkinson's and Alzheimer's) and type 1 diabetes (Jovic et al., 2022). MSCs therapy has been investigated clinically for a wide range of ailments, such as neurological damage, musculoskeletal problems and autoimmune diseases, with generally positive safety profiles documented thus far.

A comprehensive analysis of MSC transplantation in ischemic stroke, multiple sclerosis and traumatic spinal cord injury, for instance, indicated that while its efficacy is yet unknown, MSC treatment is generally safe (Kvistad et al., 2022). According to other research, MSC therapy might be a secure and practical substitute for treating chondral injuries and osteoarthritis (OA). In patients with knee OA, sophisticated MSC-based treatments have been shown to reduce pain more effectively than placebo or visco supplementation, with long-lasting benefits lasting up to a year (Tabet et al., 2024). Nevertheless, a number of further investigations have shown that the secretion of trophic (regenerative) substances plays a major role in mediating the biological and regenerative characteristics of MSCs. These elements have anti-inflammatory properties, control cell division and proliferation, and promote cell-to-cell communication. MSCs have demonstrated a remarkable capacity to influence both innate and adaptive immune responses through the release of growth factors, cytokines and extracellular vesicles (EVs). These results demonstrate a complex network of interactions between MSCs and immune cells and are corroborated by *in vitro* and *in vivo* research as well as clinical data (Jovic et al., 2022). Building on the regenerative and immunomodulatory properties of MSCs, growing evidence indicates that many of their therapeutic effects are mediated by their secreted extracellular vesicles (EVs), which represent a cell-free alternative capable of modulating redox balance, inflammation and tissue repair (Dabrowska et al., 2021).

1.7 Extracellular Vesicles in Cell Communication and Therapy

All cells, including MSCs, release a broad and heterogeneous spectrum of nanoparticles known as extracellular vesicles (EVs). Their diameter, which ranges from 30 to 1000 nm, allows them to be extensively classified. Intercellular communication depends on the proteins, lipids, mRNA and microRNA that are carried by EVs (Sharma et al., 2022). During their journey through the extracellular environment, EVs shield their cargo from enzyme destruction. Through post-translational regulation of target mRNAs and de-novo translation, EVs contents can control gene expression after their functionally active mRNA and microRNA load is released inside the recipient cell. During development and the stress

response, changes in miRNA levels are especially significant. EVs may contribute to the interchange of these molecules between cells and can potentially influence cells by activating particular signaling pathways. EVs can generate certain phenotypic alterations by changing the transcriptome and signaling activity inside recipient cells (Mulcahy et al., 2014). The role of EVs in senescent cells has been shown in numerous recent research. Compared to growing cells, senescent cells release more EVs. Other cells may be impacted by circulating EVs generated from senescent cells. EVs produced from senescent cells are therefore included in the SASP. Furthermore, EVs released by cells under specific circumstances have the potential to influence rejuvenation by influencing senescent cells (Oh et al., 2022). It is widely believed that MSC treat disease via stimulating host cells and secreting paracrine substances, as opposed to directly engrafting and replacing cells. In this regard, there is mounting evidence of the importance of extracellular vesicles (EVs) produced by stem cells, which transport and convey signaling lipids, cytokines, growth factors and regulatory miRNAs. Consequently, as recently reviewed, MSC-EVs offer a promising therapeutic agent (Mushahary et al., 2018). Exosomes have shown therapeutic benefits in several domains, such as skin and bone regeneration and the restoration of heart function. MSC-EVs have been demonstrated to promote dermal fibroblast proliferation, suggesting that they have the capacity to promote cellular proliferation and aid in the healing of wounds (Lee et al., 2023).

2. AIM OF THE STUDY

Aging and cellular senescence are two closely interconnected biological process. Cellular senescence is a protective response activated under conditions of cellular stress, such as oxidative stress, to preserve organismal homeostasis. However, the accumulation of senescent cells over time contributes to premature tissue aging and promotes the development of age relate-disease. The aim of this study is to elucidate the effect of two molecules that have previously demonstrated protective properties, in order to assess their potential to mitigate oxidative-stress-induced cellular damage and senescence. Homotaurine, is well-known for its neuroprotective properties but its effect on MSCs function and osteogenic potential has not yet been examined. Similarly, GSH, a key antioxidant molecule, may protect MSCs from oxidative stress, but its role in modulating neurodegeneration-associated pathways requires further investigation.

The first goal of the study was to assess whether homotaurine can counteract age-related alterations in MSCs, particularly enhancing their ability to differentiate into bone-forming cells. Additionally, its neuroprotective effect was evaluated using 3D Parkinson's disease organoid model, providing a unique perspective on a dual action that supports both bone regeneration and neuronal protection.

The second goal focused on the antioxidant role of GSH. Using MSCs *in vitro*, we examined its impact on cell viability, ROS levels and ROS-induced autophagy. Finally, was explored the potential of MSC-EVs as mediators of GSH effect. EVs collected from GSH-treated and untreated MSCs were applied to SH-SY5Y to determine whether they can modulate intracellular ROS levels, in order to evaluate a mechanism by which MSCs may convey protective signals to other cell types. Overall, this research aimed to provide a comprehensive proof-of-concept for the use of homotaurine and GSH as modulators of MSC function, bone regeneration and neuroprotection. By combining *in vitro*, *in vivo* and organoids models, the study seeks to uncover new therapeutic strategies that simultaneously promote skeletal and neuronal health, addressing a largely unexplored area in biomedical research.

3. MATERIALS AND METHODS

3.1 Cell Cultures

3.1.1 Mesenchymal stem cells (MSCs)

Human mesenchymal stem cells (MSCs, C-12974- PromoCell, Heidelberg, Germany) were plated at a density of $5x10^4$ cells/cm^2 and incubated at 37°C in atmosphere with 5% CO_2. Cells were cultured with MesenPro Basal medium (Gibco, Thermo Fisher Corporation, Waltham, MA, USA), supplemented with 2% of MesenPro Growth Supplement (Gibco, Thermo Fisher Corporation, Waltham, MA, USA), 1% penicillin/streptomycin/amphotericin B (PSA, Lonza, Walkersville, MD, USA) and 1% L-glutamine (Merck, Darmstadt, Germany). The completed medium was changed every 2 days after a brief wash with PBS.

3.1.2 SH-SY5Y

Human neuroblastoma cells (SH-SY5Y) were acquired from ECACC (European collection of cell culture). Were cultured in DMEM/F-12 growth medium (Thermo Fisher Scientific, Waltham, MA, USA) completed with 10% FBS (Sigma Aldrich) and 1% PSA (Lonza). The completed medium was changed every 2 days after a brief wash with PBS.

3.1.3 Treatments

The concentration of Homotaurine (lot: 200029216, code: 2200000006; Laborest S.r.l., Assago, MI, Italy) or GSH (lot: 2000025006, code: 1000000001938; Laborest S.r.l., Assago, MI, Italy) were chosen according to the literature or after CCK-8 assay at different concentrations.

3.2 Generation of mid-brain organoids

The culture media were prepared according to the protocol described by Zagare et al, 2021.

Media:

N2B27 basal medium: DMEM HAM's F12 medium (Invitrogen, ThermoFisher) - 48 mL + Neurobasal medium (Invitrogen) - 48 mL + GlutaMAX (ThermoFisher, 2mM)- 1 mL + Pen/Strep (Invitrogen, ThermoFisher) - 1 mL + N2 (17502001, ThermoFisher) -500 μL + B27 (12587-010, Invitrogen, ThermoFisher) - 1 mL.

N2B27 maintenance medium: N2B27 base medium – 10 mL + Ascorbic acid (Sigma, 20 mM) – 75 μL + CHIR (Axon MedChem, 6 mM in DMSO) – 5 μL.

N2B27 pattering medium: N2B27 base medium – 10 mL + hBDNF (Pepotech, 10 mg/mL) – 10 μL + hGDNF (Pepotech, 10 mg/mL) – 10 μL + Ascorbic Acid (Sigma, 20 mM) – 100 μL + + TGF 3 (Pepotech10 ng/uL) 1 ng/mL - 1 μL + db cAMP (Pepotech100 mM in milliQ H2O) - 50 μL + PMA (stock 10mM) 1μL.

N2B27 differentiation medium: N2B27 base medium - 10 mL + hBDNF (Pepotech,10 mg/mL) - 10 µL + hGDNF (Pepotech,10 mg/mL) -10 μL + Ascorbic acid (Sigma, 20 mM) - 100 µL + TGF 3 (Pepotech10 ng/µL) 1 ng/mL- 1 μL + db cAMP (Pepotech100 mM in milliQ H2O) - 50 µL.

Neuronal epithelial stem cells (NESCs) were generated from human-induced pluripotent stem cells (iPSC) (A13777, Gibco-ThermoFisher) which carried the LRRK2 (leucine-rich repeat kinase 2)-G2019S mutation. NESCs were cultured in Geltrex-coated 6-well plates and routinely passaged upon reaching 80-90% confluence, using Accutase (Sigma-Aldrich, St. Louis, MO, USA). For the initiation of 3D cultures, 9.0 x 10^5 cells were resuspended in 15 mL of N2B27 maintenance medium. A volume of 150 μL of this suspension was plated into each well of a 96-well ultra-low attachment (ULA) plate (7007, Corning-ThermoFisher Corporation, Waltham, MA, USA). After two days, N2B27 maintenance media was replaced with N2B27 pattering media.

Out of 16 organoids generated, 8 were destinated for embedding protocol, while the other 8 were kept as non-embedded organoids for molecular analyses.

The day 8, N2B27 pattering medium was substituted with N2B27 differentiation medium, and treatment with Homotaurine (0,25 mM) was started. 8 3D colonies were transferred to an untreated 24-well tissue culture plate (TCP), each well containing 500 μL of pre-warmed N2B27 maintenance medium. Each colony was embedded in a 30 μL geltrex droplet,

ensuring central positioning within the hydrogel. Geltrex was incubated for 25 min at 37°C, after which the medium was replaced with N2B27 with or without Homotaurine.
Cultures were maintained for 40 days, medium was changed every 3-4 days using 500 μL of N2B27 differentiation medium, with or without treatment. At the end, non-embedded organoids were collected in Eppendorf and stored at -80°C, for RNA and proteins extraction. Embedded organoids were processed for sectioning and immunostaining.

3.2.1 Midbrain organoid size measurement

Size of the midbrain organoids was measured during differentiation to assess the morphological changes. Images were acquired for each condition using a stereomicroscope SMZ25 (Nikon, Minato-Tokyo, Japan) and analyzed with NIS imaging software version 6.10.01 (Nikon, Minato-Tokyo, Japan).

3.2.2 Confocal Analysis of NESCs 3D Colonies

NESCs 3D colonies were fixed in 4% paraformaldehyde (PFA; P6148, Sigma-Aldrich St. Louis, MO, USA), embedded in 3% agarose and cut into 70 μm sections using a Vibratome (Leica). The resulting slices were transferred into 24-well plates filled with PBS (Gibco, Thermo Fisher Scientific, Waltham, MA, USA).
For immunolabeling, the slices were first permeabilized with 0.5% Triton X-100 (Sigma Aldrich, St. Louis, MO, USA) in PBS for 30 min at room temperature (RT) on a shaker. Then, sections were washed two times in 0,01% Triton X-100 in PBS for 5 minutes. Samples were incubated in a blocking solution for 2h at RT. Primary antibodies (Table 1) were added and allowed to bind for 48h at RT.

Primary Antibody	Dilution	Origin	Secondary Antibody Fluorophore
TH	1:1000	Cell Signaling	Anti-rabbit (Alexa568)
GFAP	1:1000	Cell Signaling	Anti-chicken (Alexa488)
MAP2	1:500	Cell Signaling	Anti-mouse (Alexa647)

Table 1: *Neuronal markers for confocal imaging.*

After primary antibody incubation, sections were washed three times with 0.01% Triton X-100 in PBS for 10 minutes each at RT on a shaker. Secondary antibodies (Table 1) were applied for 2h at RT on a shaker.

The slices were washed again three times for 10 min with 0.01% Triton X-100 in PBS at RT, followed by a final rinse in milliQ. The stained sections were gently lifted using a fine brush and placed onto microscope slides with a printed grid. To prevent movement during mounting, the sections were allowed to partially air-dry before the addition of the mounting medium and placement of the cover glass. The intermediate filament-III protein GFAP is only present in enteric glial cells, non-myelinating Schwann cells in the peripheral nervous system and astrocytes in the central nervous system. Its expression can be altered by numerous substances, such as growth factors, lipopolysaccharides and nuclear-receptor hormones.

Tyrosine hydroxylase (TH) is expressed in neurons and endocrine cells that contain dopamine, norepinephrine and epinephrine (catecholamine), but its expression is high during the development of these cells while in adulthood, they stop expressing TH or only express it extremely weakly.

Neuronal development, differentiation and plasticity are all significantly influenced by MAP2. It plays important roles in how neurons react to neurotoxins, growth factors, neurotransmitters and synaptic activity. Midbrain organoids generated from iPSCs with the LRRK2-G2019S mutation (MUT) were used in this investigation. The identical iPSCs that had undergone gene correction into the wild type form (GC) were utilized as the control. Therefore, in the organoids produced from the GC and MUT T413 cell lines, these three markers were fluorescently labeled and seen using confocal microscopy.

Confocal imaging (Leica Wetzlar, Germany) was used to detect the three neuronal markers, and fluorescence positive regions were evaluated semi-quantitatively using imageJ software.

3.3 CCK-8 assay

Cell viability was verified by using Cell Counting Kit-8 (CCK-8, Immunological Science Rome, Italy), following the manufacturer's instructions. MSCs and SH-SY5Y cells were seeded in 96-well plates. MSCs were plated at a density of 3.0 x10^4 cells for well and allowed to adhere overnight before treatment. A density of 10.0 x10^4 cells for well was plated for SH-SY5Y cells and the treatment was performed after 48h. Treatments are described in table 2.

Model	Treatment category	Treatment conditions	Time point
MSCs	Homotaurine	-CTRL -Homotaurine (100 μM)	24h, 3, 7, 24, 21 days
MSCs	GSH	-CTRL (untreated) -H_2O_2 (350 μM) -TBHP (100 μM) -GSH (2 mM) -H_2O_2 (350 μM) + GSH (2 mM) - TBHP (100 μM) + GSH (2 mM)	24h
SH-SY5Y	GSH	-CTRL (untreated) -H_2O_2 (350 μM) -TBHP (100 μM) -GSH (2 mM) -H_2O_2 (350 μM) + GSH (2 mM) - TBHP (100 μM) + GSH (2 mM)	24h
SH-SY5Y	EVs	- CTRL- EVs + CTRL - GSH - EVs + CTRL - CTRL- EVs + H_2O_2 - GSH - EVs + H_2O_2	24h

Table 2: *Cell type analyzed, the experimental treatments applied and corresponding time points.*

CCK-8 assay procedure:

After the corresponding treatments, the medium was removed and a wash with PBS was done. Then, the medium with 10% of CCK-8 solution was added to each well. The absorbance was measured at 450 nm with Tecan Infinite M200 (Tecan, Männedorf, Switzerland) immediately after (t0) and each hour for other three times (t1, t2, t3).

Cell viability was expressed as a percentage relative to untreated CTRL group and was calculated using the following equation:

$$Cell\ viability\ (\%) = \frac{A_{treated}}{A_{control}} x100$$

3.4 ROS assay

For the detection of reactive oxygen species (ROS) levels distinct protocols were employed for MSCs, NESC organoids and SH-SY5Y. The table 3 shows the cell types and the protocols applied.

Cell Model	Method	Probe	Instrument
MSCs	Flow cytometry	CellROX™ Deep Red (Invitrogen)	BD Accuri™ C6
NESC organoids	Flow cytometry	DCFDA (Sigma)	BD LSRFortessa™ X-20
MSCs; SH-SY5Y	Microplate fluorimetry	DCFDA Kit (Abcam)	Victor X4 (PerkinElmer)

Table 3: *Cell models, detection methods, probes and instruments used in the study.*

ROS detection in MSCs treated with Homotaurine:

ROS quantification in MSC was performed using CellROX™ Deep Red (Cat. C10422; Invitrogen, Waltham, MA, USA). Cells were seeded in a 6-well plate at a density of 3.0 x 10^5 cells/well and cultured in MesenPro medium (PromoCell), with or without Homotaurine (100 μM). Analyses were carried out at five time point: 24h, 3, 7, 14 and 21 days. For each time point cells were washed with PBS, detached and counted. Then, 10.0 x 10^5 were incubated with 2 μM CellROX™ Deep Red for 30 min at 37°C. After incubation, cells were washed in PBS and immediately analyzed using BD Accuri™ C6 (BD Biosciences, Franklin

Lakes, NJ, USA). Fluorescence intensity values were used to quantify intracellular ROS production at each time point.

ROS detection in NESC Organoids:

ROS levels in NESC-derived organoids were measured using DCFDA (2',7'-dichlorofluorescein diacetate) (Cat. D6883; Sigma, St. Louis, MO, USA).

For each condition 8 organoids were pooled and were incubated in Accutase (A6964-500M, Sigma) for 20-30 min to detach the entire network as a single structure. After, cells were centrifuged at 400 xg for 5 min and washed with 1% BSA in PBS. Cells were then incubated with 5 μg/mL DCFDA in fresh medium for 30 min. After staining, cells were transferred to FACS tubes and analyzed using BD LSRFortessa^{TM} X-20 (BD Biosciences, Franklin Lakes, NJ, USA). Dead cells were excluded using propidium iodide (PI) staining (Cat. BMS500PI; eBioscience ThermoFisher, Waltham, MA, USA).

For both MSCs and NESC organoids analyzed by flow cytometry, untreated cells were used to establish background fluorescence levels. Flow cytometry data were analyzed using FlowJo v10.

ROS detection in MSCs and SH-SY5Y treated with GSH and oxidative stressors:

For experiments involving GSH, ROS levels were quantified using the DCFDA/H2DCFDA Cellular ROS Assay Kit (ab113851, Abcam Cambridge, MA, UK). MSC and SH-SY5Y were seeded in 96-well plates at densities of 3.0 x 10^3 and 1.0 x 10^4 per well, respectively. Cells were washed with PBS and incubated with 10 μM DCFDA solution for 45 min at 37°C in the dark. After a brief wash with PBS, the treatment media were added (Table 4).

Model	**Treatment category**	**Treatment conditions**
MSCs	GSH	-CTRL (untreated) -H_2O_2 (350 μM) -TBHP (100 μM) -GSH (2 mM) -H_2O_2 (350 μM) + GSH (2 mM) - TBHP (100 μM) + GSH (2 mM)

SH-SY5Y	GSH	-CTRL (untreated) -H_2O_2 (350 μM) -TBHP (100 μM) -GSH (2 mM) -H_2O_2 (350 μM) + GSH (2 mM) - TBHP (100 μM) + GSH (2 mM)
SH-SY5Y	EVs	- CTRL- EVs + CTRL - GSH - EVs + CTRL - CTRL- EVs + H_2O_2 - GSH - EVs + H_2O_2

Table 4: *Cell types and treatments applied.*

Fluorescence was measured using Victor X4 (PerkinElmer) at Ex 485 nm/Em 535 nm. Relative ROS levels were calculated by normalizing fluorescence values to untreated CTRL.

3.5 Protein extraction and quantification

Protein extraction was performed on cell cultures and NESC organoids. After treatment, cells and NESCs organoids were collected and stored at -80 °C. Pellet were lysed in RIPA buffer (Cat. 89900, Thermo Fisher Scientific, Waltham, MA, USA) supplemented with Protease Inhibitor Cocktail (Cat. 78429; ThermoFisher). Briefly, after the addition of RIPA buffer, the homogenate pellet was incubated for 30 minutes on ice. Then, samples were centrifugated at 16000 xg at 4°C for 40 min.
Proteins were quantified using BCA assay (Thermo Scientific, Waltham, MA, USA), following the manufacturer's instruction and read at 560 nm with Victor X4 (PerkinElmer).

3.6 Western Blotting analysis

Equal amount of protein sample was denaturized by adding Loading Buffer and boiled ad 99°C for 7 minutes. Then proteins were separated on 10% or 14% sodium dodecyl sulfate-polyacrylamide gel electrophoresis (SDS-PAGE). Gels were immersed in Running Buffer solution 1X during the electrophoresis run, set at 125 V for the first 15 minutes and changed to 145 V until the run was completed.

Following electrophoretic separation, proteins were transferred onto polyvinylidene difluoride (PVDF) with a pore size of 0.45 μm (Thermo Fisher Scientific, Waltham, MA, USA). PVDF membranes were activated with ethyl alcohol for 2 minutes and then washed with millQ water for 5 minutes. After wash membranes were incubated in Transfer Buffer 1X. The transfer was carried out using (Mini-PROTEAN® Tetra Cell, 4-Gel System, Bio-Rad) at an electric current of 80 V for 2 hours, allowing proteins to pass from the gel to the membrane. After transfer, membranes were stained with Amido Black (Cat. Number A8181-Sigma-Aldrich-St.Louis, Missouri, USA) for 1 minute, then membranes were washed with milliQ water.

Membranes were blocked with fat-dry milk diluted at 5% in TBS-Tween at room temperature for 1 hour to reduce nonspecific antibody binding. After blocking, membranes were incubated with primary antibodies overnight at 4°C (Table 5).

Ab I	Dilution	WM	Origin	Ab II
SESN1	1:1000	57 kDa	PA5-98142, Invitrogen	Anti-rabbit
SESN2	1:1000	54 kDa	ab-178518, Abcam	Anti-rabbit
p53	1:1000	53 kDa	9282, Cell Signaling	Anti-rabbit
p21	1:1000	21 kDa	2947, Cell Signaling	Anti-rabbit
RUNX 2	1:1000	55-62 kDa	12556, Cell Signaling	Anti-rabbit
β- catenin	1:1000	85 kDa	PA5-19469, Invitrogen	Anti-rabbit
P- β-catenin	1:1000	92 kDa	95615, Cell Signaling	Anti-rabbit
LC3B	1:1000	14-16 kDa	2775, Cell Signaling	Anti-rabbit
p62	1:1000	47 kDa	600-401-HB8, Rockland	Anti-rabbit
β-actin	1:10000	42 kDa	MA1-140, Invitrogen	Anti-mouse

Table 5: *List of primary antibodies used with their dilutions and molecular weight.*

Following primary incubation, membranes were washed with TBS-Tween 3 times for 10 minutes. Then, membranes were exposed to secondary antibodies (Table 6) for 1 hour at room temperature. Subsequently, membranes were washed another 3 times with TBS-Tween solution.

AbII	Dilution	Origin
Anti-rabbit	1:1000	7074, Cell Signaling
Anti-mouse	1:4000	7076, Cell Signaling

Table 6: *List of secondary antibodies used and their dilutions.*

Signal acquisition was performed through the use the ECL Select Western Blotting Detection Reagent Kit (Amersham, Cytiva) to find the protein signal at the UVITEC imager (Alliance).

3.7 RNA extraction and reverse transcriptions

Samples were collected and stored at -80°C until the use. Then, total RNA was extracted using the RNeasy® protect mini kit (Qiagen, Hilden, Germany) according to the manufacturer's instruction. The quantity and quality of RNA were verified using a Qubit 3 Fluorometer (Thermo Fisher Scientific, Waltham, MA, USA). For reverse transcription, 150 ng of total RNA from organoids samples and 500 ng from zebrafish samples were used. Reverse transcription was performed with High-Capacity cDNA reverse transcription kit (Thermo Fisher Scientific, Waltham, MA, USA) as detailed in the accompanying table 7. The 2X RT master mix was prepared on ice, added to RNA and the reverse transcription was carried out using a thermocycler (Bioer Technology, Hangzhou, China). The cDNA was used for Real-Time quantitative PCR (RT-qPCR) analysis.

Reagent	Quantity for each sample
10X RT Buffer	2 µL
10x RT Random Primers	2 µL
dNTO mix (100 mM)	0,8 µL
MultiscribeTM Reverse Transcriptase	1 µL
H_2O RNAse free	4,2 µL

Table 7*: List of reagents and their respective quantities used in Reverse Transcription.*

3.8 Real-Time quantitative PCR

3.8.1 Taqman Real-Time PCR

RT-qPCR was performed to assess gene expression levels. Each PCR reaction was performed using TaqMan Universal PCR Master Mix (Thermo Fisher Scientific, Waltham, MA, USA), with 2 µL of cDNA for sample in a total volume of 20 µL (see Table 8).
β-actin was used as housekeeping gene and was conjugated to the fluorophore VIC, while CTNN1 was conjugated to carboxyfluorescin (FAM).

Reagent	Quantity for each sample	Origin
TaqMan® Universal PCR Master Mix	10 µL	Applied Biosystems, Thermo Fisher
Taqman Target Gene CTNNB1 (Hs00355045_m19)	1 µL	Thermo Fisher Scientific
Housekeeping Gene *β-actin* (Hs99999903_m1)	1 µL	Thermo Fisher Scientific
H_2O RNase free	6 µL	

Table 8: *List of reagents and their respective quantities used in TaqMan Real-Time PCR.*

Three copies for each sample were loaded to the MicroAmp optical 96-Well Reaction Plate (Applied Biosystems, Life Technologies), after a brief centrifugation, the plate was covered and sealed using the proper membrane (OPTI-SEAL, AB ANALITICA). The samples were amplificated by LineGene 9620 Real-Time PCR System (Bioer Technology, Hangzhou, China), the thermal cycling conditions are reported in Table 9 and repeated 45 times.

Step	Temperature	Time
Step 1	95°C	10 minutes
Step 2	95°C	15 seconds
Step 3	60°C	1 minute

Table 9: *Steps of TaqMan Real-Time PCR reaction in LineGene 9620 Real-Time PCR Systems.*

Fluorescence signals generated during the real-time PCR reactions were quantified using the ΔCt (Delta Ct) method, following standard comparative threshold cycle analysis.

3.8.2 Sybr Green Real Time

The SYBR Green Real-Time PCR was realized using SYBR™ Green PCR Master Mix (Applied Biosystems, Thermo Fisher Scientific) in singleplex. The mixture contained both forward and reverse primers, diluted in H_2O RNAse free at a ratio of 1:10, for every target gene. The analysis was performed using 20 ng of cDNA in a total reaction volume of 20 µL. The components of the mix are listed in the following table 10.

Reagent	**Quantity for each sample**
SYBR™ Green PCR Master Mix (Applied Biosystems, Thermo Fisher Scientific. Ref: 4309155)	10 µL
Primer forward	0,6 µL
Primer reverse	0,6 µL
H2O RNAse free	6,8 µL

Table 10: *Reagents and their quantities used for SYBR Green Real-Time PCR.*

Triplicates were loaded in 96-Well Reaction Plate (Applied Biosystems, Life Technologies) and amplificated by LineGene 9620 Real-Time PCR System (Bioer Technology, Hangzhou, China). The thermal cycling conditions are reported in Table 11 and repeated 45 times.

Step	**Temperature**	**Time**
Step 1	95°C	3 minutes
Step 2	95°C	10 seconds
Step 3	53-61°C (based on primers' Melting Temperature)	30 seconds
Step 4	72°C	30 seconds
Step 5	95°C	10 seconds
Step 6	50°C	5 seconds
Step 7	95°C	15 seconds

Table 11: *Steps of SYBR Green PCR reaction in LineGene 9620 RealTime PCR Systems.*

Genes analyzed are included in Table 12.

Gene	Origin	Primers
RUNX 2a	Invitrogen	Fw: GACGGTGGTGACGGTAATGG, Rv: TGCGGTGGGTTCGTGAATA
RUNX 2b	Invitrogen	Fw: CGGCTCCTACCAGTTCTCCA, Rv: CCATCTCCCTCCACTCCTCC
CTNNb1 (Danio Rerio)	Invitrogen	Fw: ATTGTGGAGGCTGGTGGC, Rw: CCCTCCTGTTTGGTGGCG
Sp7	Invitrogen	Fw: GGCTATGCTAACYGCGACCTG, Rw: GGCTATGCTAACTGCGACCTG

Table 12: *List of genes analyzed trough SYBR Green Real-Time PCR reaction.*

Fluorescence signals obtained from the real-time PCR assays were quantified using the ΔCt method.

3.9 Zebrafish

Zebrafish experiments were realized at the Interdepartmental Centre of Experimental Research Service (CIRSAL), University of Verona, Italy, in accordance with the approved experimental protocol issued by the Directorate-General for Animal Health and Veterinary Medicinal Products of the Italian Ministry of Health (authorization code 447/2023-PR). Fish were randomly selected based on age and the sample size was defined to ensure adequate statistical power. Animals showing signs of suffering were excluded from the study. Embryos were obtained from KDRL-GFP zebrafish, which express green fluorescent protein (GFP) under the control of the KDR (kinase insert domain receptor) promoter. Embryos were maintained at 33° C in water supplemented with 0.25 mM homotaurine starting from 2 days post-fertilization (2 dpf) (Control n=90; treated n=90). Homotaurine exposure was continued for 14 days, up to the final experimental stage at 16 dpf. Adult (4 months old; CTRL n=7; treated n=8) and aged (36 months old; CTRL n=3; treated n=3) zebrafish were kept in water containing or not 0.25 mM homotaurine for 7 days. At the end of treatment period, fish were euthanized and collected for molecular analyses. Using the transgenic KDRL-GFP zebrafish line, we examined how homotaurine affected angiogenesis in an elderly model. In zebrafish research, the KDRL-GFP (kinase insert domain receptor-like–enhanced green fluorescent protein) model is frequently used to examine vascular

development and angiogenesis. To visualize GFP fluorescence in living animals, the promoter of the kinase insert domain receptor-like (KDRL gene), which codes for a receptor similar to human vascular endothelial growth factor receptor 2 (VEGFR2), was fused to GFP in this transgenic model.

Since the intensity of GFP fluorescence is directly proportional to the levels of KDRL gene expression, this allows for the visualization of blood vessel formation and vascular patterning in vivo as it takes place during development or in response to experimental treatments.

Fluorescence imaging was performed using a Leica M205FA fluorescence microscope (Leica Microsystems, Wetzlar, Germany). Quantification of fluorescent area was carried out with ImageJ software (version 1.54m).

3.10 Extracellular vesiscles isolation and quantification

Extracellular vesiscles (EVs) were isolated from the conditioned medium of MSCs cultured under two experimental conditions: control MSCs and MSCs treated with GSH (2mM).

MSCs were cultured in T175 flask with DMEM completed with 1% PSA and 3% FBS. Specifically, FBS was previously ultra centrifugated at 100000 xg at 4 °C for 18 hours with Optima XPN-80 Ultracentrifuge (Beckman Coulter, Cassina de' Pecchi, MI, Italy).

After 24 h of incubation, the conditioned medium was collected and subjected to centrifugations to remove cells and debris. First, the medium was centrifuged at 400 xg for 1° minutes at 4 °C. The supernatant was transferred to clean tubes and centrifuged at 2000 xg for 30 minutes at 4 °C. The resulting supernatant was subsequently processed by ultracentrifugation. EVs were pelleted by a first ultracentrifugation step at 100000 xg for 1h 30 minutes at 4 °C. The pellets were washed by resuspension in PBS and subjected to a second ultracentrifugation at 100000 xg for 1h 30 minutes to remove contaminating and soluble factors. At the end EVs were resuspended in PBS until quantification and further analyses. EVs concentration and size distribution were assessed by Nanoparticle Tracking Analysis (NTA) using Nano Sight NS300 (Malvern Panalytical, Lisson, MB, Italy). Samples were diluted in sterile PBS to reach the optimal particle concentration range and analyzed under constant camera settings. Three videos of 60 seconds each were recorded for sample and data were processed using the manufacturer’s software.

3.11 Characterization of EVs

3.11.1 MACSPlex Multiplex Characterization

EVs surface marker profiling was performed using MACSPlex Exosome Kit (Miltenyi Biotec, Bergisch Gladbach, Germany), following the manufacturer's instructions. 1 x 10^8 EVs for condition and a blank control, were incubated with 15 μl of MACSPlex EV IO Capture Beads in an orbital shaker overnight. After incubation samples were washed with MACSPlex Buffer. Then, samples were incubated with EV IO Dectection Reagent for CD9, CD63 and CD81 for 1 hour protected from light in an orbital shaker at room temperature. Then, samples were washed two times with MACSPlexBuffer and analyzed using BD FACSFortessa™ flow cytometer. Median fluorescence intensities (MFI) were analyzed using FlowJo software (BD Biosciences).

3.11.2 Transmission electron microscopy (TEM)

25 µl of each sample was placed on a 400 mesh holey film grid; samples were stained with 2% uranyl acetate for 1 minute and then were observed with a Tecnai G2 (FEI) transmission electron microscope operating at 100 kV. 20 Images for each condition were captured with a Veleta (Olympus Soft Imaging System) digital camera.

3.12 Cellular staining

SH-SY5Y were plated in 6-well in their basal media, with FBS depleted of EVs. Cells were stained with a vital fluorescent dye, the Vybrant Cell Labeling Solution (Invitrogen, Waltham, MA, USA), using 3,3′-dioctadecyloxacarbocyanine perchlorates (DiO), which emits green fluorescence at 501 nm. The cell nuclei were stained with Hoechst dye (Thermo Fisher Corporation, Waltham, MA, USA). EVs were stained with 1,1′-dioctadecyl-3,3,3′,3′-tetramethylindocarbocyanine perchlorate (DiI), a red fluorescent dye with emission at 565 nm and added to the cells for conditioning. After 18 hours cells were visualized using EVOS M5000™ Core Imaging System (Invitrogen, Thermo Fisher Scientific, Waltham, MA, USA).

3.13 Statistical analysis

Statistical analyses were performed using SPSS for Windows, version 22.0 (SPSS). Data are reported as mean ± Standard deviation (SD). Differences between control groups and their corresponding experimental conditions were evaluated using a two-tailed paired Student's T-test. A p-value < 0.05 was considered statistically significant. For *in vitro* experiments, analyses were conducted on data obtained from at least three independent biological replicates.

4. RESULTS

4.1 Impact of Homotaurine on ROS Levels, Cell Viability Sestrin, p53, and p21 Levels, in senescent Mesenchymal Stem Cells

Aging has a significant impact on MSCs and is known that ROS increase with age, for this reason we investigated on ROS levels in MSCs. As it can be seen in Figure 4, we observed a marked rise in ROS levels beginning on the third day of culture and continuing to increase after day 7 (Figure 4A), which points to a possible link between increased ROS levels and the development of cellular senescence in MSCs.

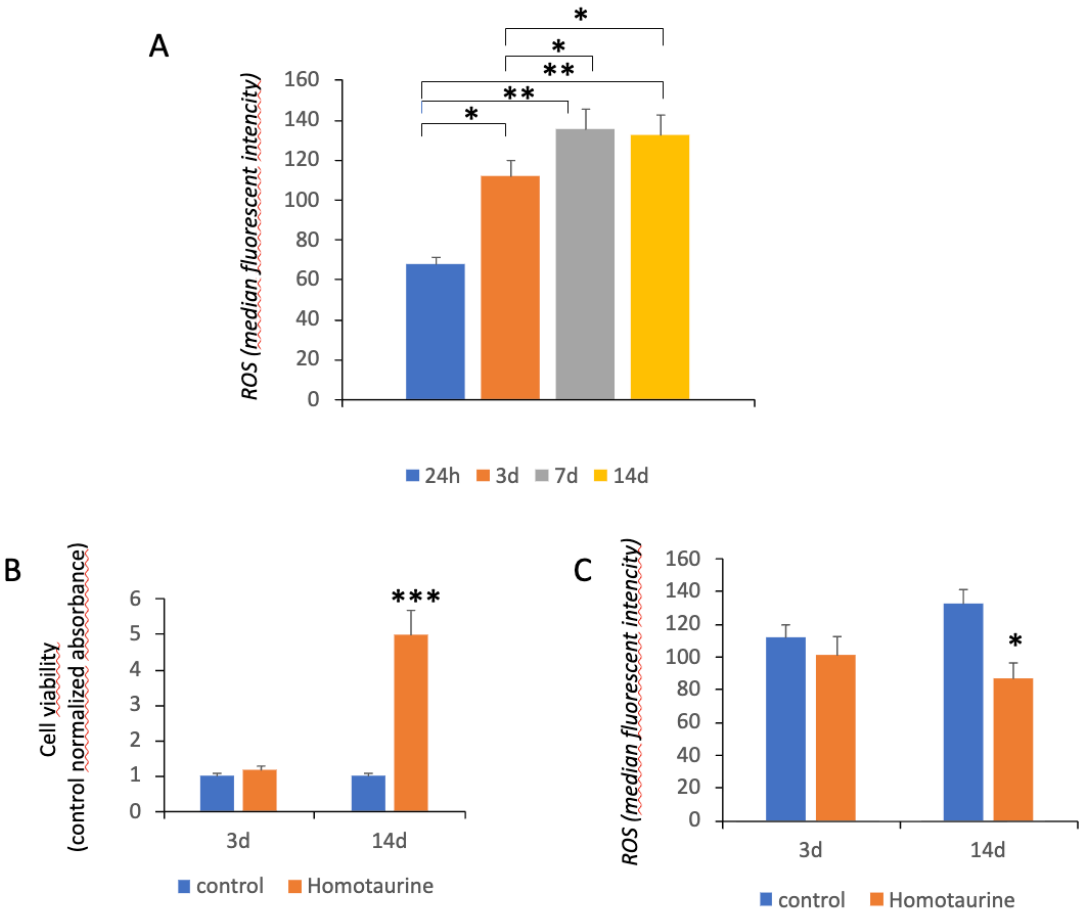

Figure 4: *Effect of homotaurine treatment on ROS levels and MSCs viability after 14 days. ROS levels showed an increase after 3 days of culture (A). Homotaurine treatment improved cell viability after 14 days (B). Homotaurine promoted a decrease in ROS levels after 14 days (C). (*p<0.05;**<0.01;***<0.005).*

Next, the attention was moved to the effect of homotaurine on MSC viability and ROS levels. When compared to untreated cells, our data showed that homotaurine administration improved cell viability on day 14 of culture, while no changes were observed after three days of culture (Figure 4B). Remarkably, under the homotaurine treatment a decrease in ROS levels was linked to the improvement in cell viability observed on day 14 (Figure 4C). After 21 days of administration, the beneficial effects of homotaurine on cell viability were also observed, as improved cell viability was a result of homotaurine treatment (Figure 5A).

Then we examined levels of two proteins which are involved in controlling cellular stress responses: Sestrin 1 and 2. Sestrin 1 levels significantly increased after 24 hours but a decrease is shown after 21 days of administration. When we investigated Sestrin 2 levels neither of the two time points showed any discernible changes in its expression (Figure 5B). Since p53 and p21 are well-known regulators of the cell cycle and stress responses, we next examined their levels in cells treated with homotaurine.

Comparing the treated cells with their corresponding controls, we found that the p53 levels in the treated cells remained unchanged (Figure 5C), while MSCs treated with homotaurine showed a considerable decrease in p21 levels after 21 days (Figure 5D).

These results underline the protective role of homotaurine on stress response and cellular homeostasis.

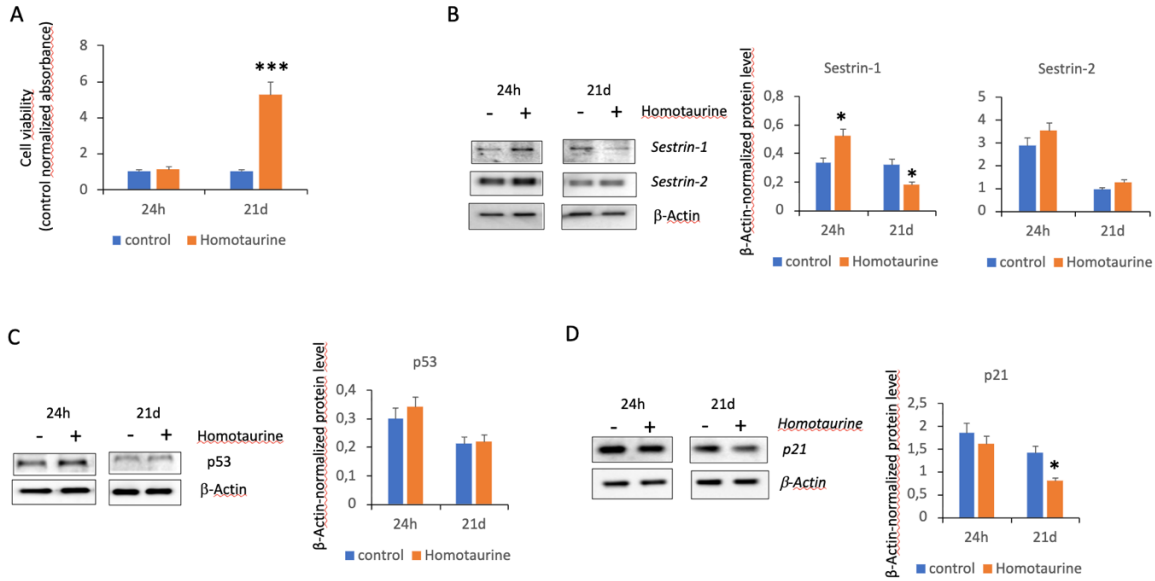

Figure 5: *Effect of homotaurine on cell viability and protein expression. Cell viability increased after 21 days of treatment (A). After 24 h of treatment a significant increase in Sestrin 1 levels were detected, however there was a decrease at 21 days of treatment, Sestrin 2 levels remained stable (B). (C) No significant differences were showed in p53 levels, while there was a reduction in p21 levels after 21 days of treatment (D). (*p < 0.05; ***p < 0.005).*

4.2 In the zebrafish model, homotaurine increases angiogenesis and promotes the expression of genes linked to osteogenesis.

MSCs are essential for maintaining skeletal homeostasis and enabling bone regeneration. So, we treated zebrafish (*Danio rerio*) larvae with or without homotaurine for 14 days. Our findings showed that the expression of the genes Runx2b, Sp7 and β-catenin, which are important regulators of osteogenesis and skeletal development, was significantly increased (Figure 6A). Furthermore, treatment with homotaurine in 4-month-old zebrafish, affected the expression of osteogenesis-associated genes β-catenin, runx2a, runx2b and sp7 (Figure 6B), suggesting a long-lasting effect on skeletal development and maintenance.

With aging, angiogenesis mechanisms are frequently compromised, resulting in a decreased vascular regeneration and repair. This reduction in angiogenic ability is a major element in the aging process overall and is linked to a number of age-related illnesses.

Therefore, we examined how aging affects angiogenesis in 36-month old KDRL-GFP zebrafish model. For seven days, 0.25 mM homotaurine was administered to the elderly fish. According to our findings, VEGFR2 expression significantly increased (Figure 6C), especially in the tail region (Figure 6D). According to these results, the homotaurine therapy increased the expression of genes linked to osteogenesis and encouraged angiogenesis in zebrafish at various stages of development.

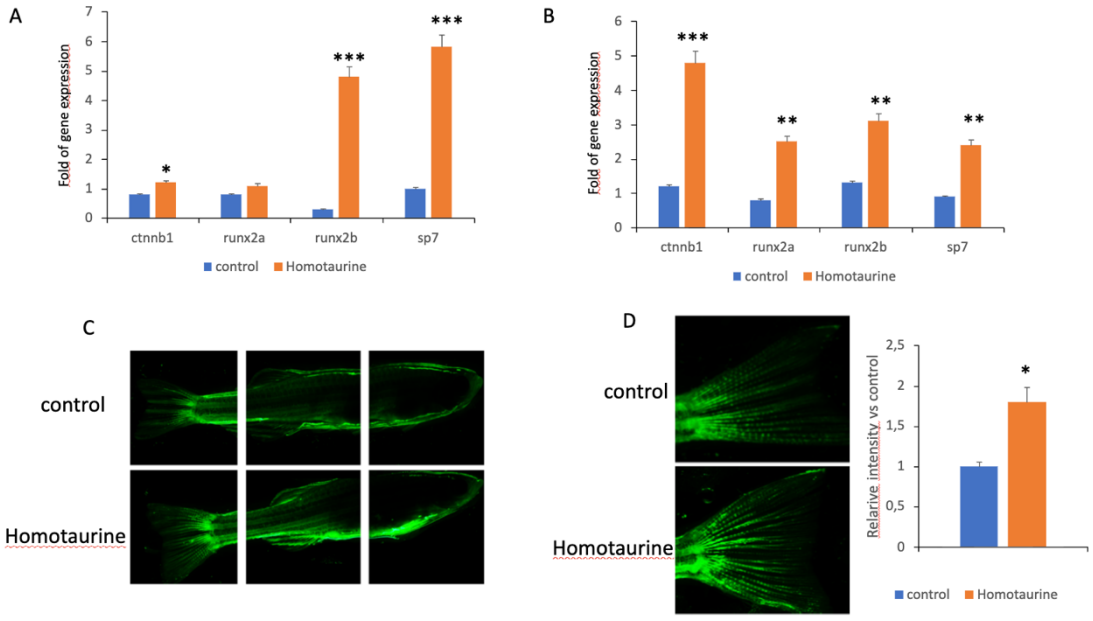

Figure 6: *Effect of homotaurine on angiogenesis and osteogenesis gene expression in Danio Rerio. Expression of genes crucial for skeletal development in zebrafish larvae treated for 14 days (A). Expression of skeletal genes in 4-month old zebrafish (B). Treatment for 7 days of homotaurine in aged zebrafish (36 months old) enhanced vascular endothelial growth factor receptor 2 (VEGFR2) (C), in particular in the tail region (D). (*p<0.05;**p<0.01; ***p<0.005).*

4.3 Homotaurine Reduces ROS Generation and Increases RUNX2 and β-Catenin in an Organoid Model of Parkinson's Disease

We investigated how homotaurine can influence 3D NESC organoid colonies that had the LRRK2-G2019S mutation, one of most the common mutation that cause Parkinson's disease. We evaluated the expression of three neuronal markers that are often downregulated in Parkinson's disease patients: glial fibrillary acidic protein (GFAP), tyrosine hydroxylase (TH) and microtubule-associated protein 2 (MAP2) (Figure 7A,B). When comparing the NESC 3D organoid colonies from the mutant T413 cell line to those from the gene-corrected counterpart, the semi-quantitative analysis showed decreases in the expression levels of all three studied neuronal markers (Figure 7C).

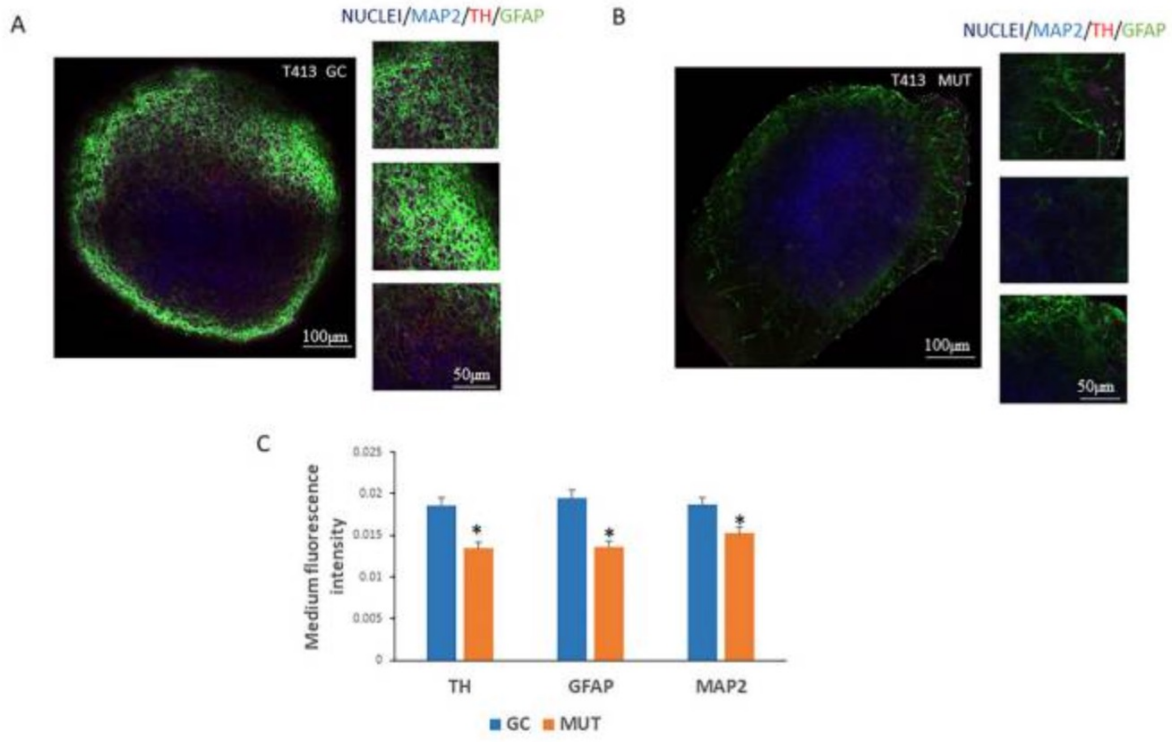

Figure 7: *Neuronal markers in 3D neuronal epithelial stem cell (NESC) organoids carrying the leucine-rich repeat kinase 2 (LRRK2)-G2019S mutation derived from induced pluripotent stem cells (iPSCs). (A) 3D NESC organoids generated from both gene-corrected (GC) and (B) mutated (MUT T413) iPSC lines were incubated with antibodies against TH, GFAP and MAP2 neuronal markers and visualized using confocal microscopy. In blue nuclei, in purple MAP2 marker, in red the TH marker and in green the GFAP marker. (C) Fluorescence for each marker was measured for the two conditions. (*p< 0.05).*

The effects of homotaurine were then assessed by treating the organoids generated from the mutant cells. We performed a thorough examination of the dimensions of eight organoids at various differentiation time points (6, 9, 28, and 40 days) in order to evaluate the possible impacts and toxicity of homotaurine (Figure 8A). As seen in Figure 8B, the colonies treated with homotaurine maintained similar dimensions to the untreated (UNTR) colonies, indicating that homotaurine has no negative effects on colony size during differentiation.
Furthermore, cytofluorimetric measurements of ROS confirmed the positive effects of homotaurine. Compared to the untreated controls, the homotaurine-treated samples showed a considerable decrease in ROS levels (Figure 8C).

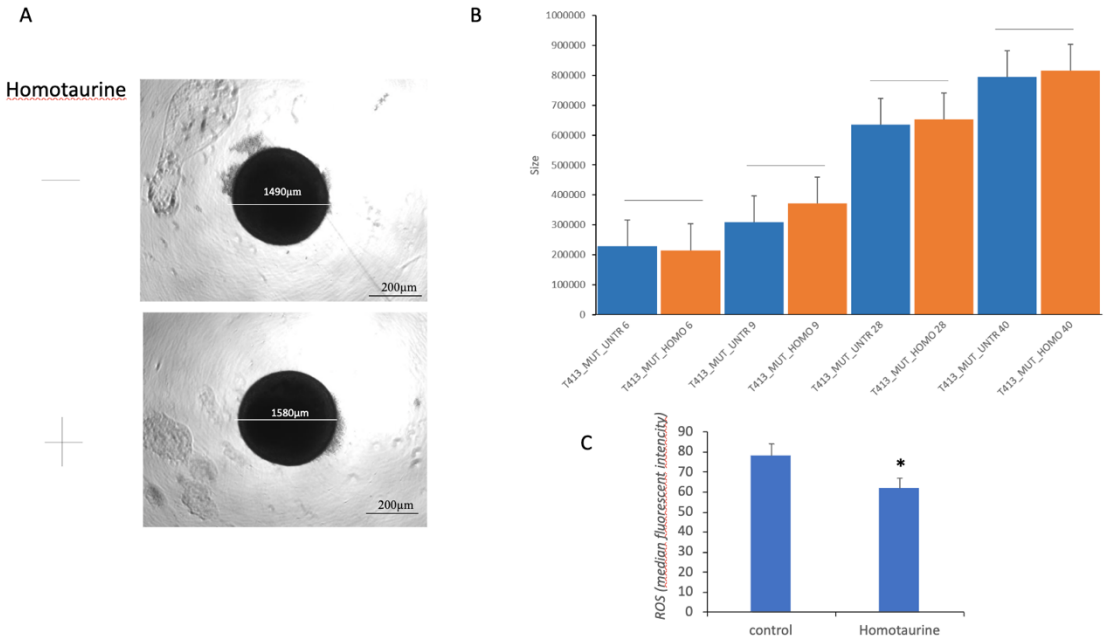

Figure 8: *Homotaurine's effects on LRRK2-G2019S mutated midbrain organoids size and ROS levels for each condition. (A) Images whit diameters of mock-treated (top) and homotaurine-treated (bottom) NESC colonies. Homotaurine didn't alter colony size compared to untreated controls, the area (size, µm^2) of LRRK2-G2019S-mutated midbrain organoids was assessed at multiple timepoints (6, 9, 28 and 40 days) (B). After 40 days, ROS levels decreased after homotaurine treatment compared to controls (C). (*p< 0.05).*

Wnt activation has been shown to decline with age, for this reason we examined how homotaurine therapy can affected the major Wnt signaling pathway effectors.

Our results suggest that the Wnt pathway was activated after homotaurine treatment. In fact, CTNNB1 gene, which codes for β-catenin, had higher gene expression levels (Figure 9A). We also examined the Runx2 levels because the Runx2 gene is a known direct target of the classical Wnt signaling pathway, which is mediated by β-catenin. Protein analysis indicated a decrease in the phosphorylated form of β-catenin and increased levels of Runx2 and total β-catenin, as seen in Figure 9B. These results also suggest that Wnt signaling activity may be increased by homotaurine treatment.

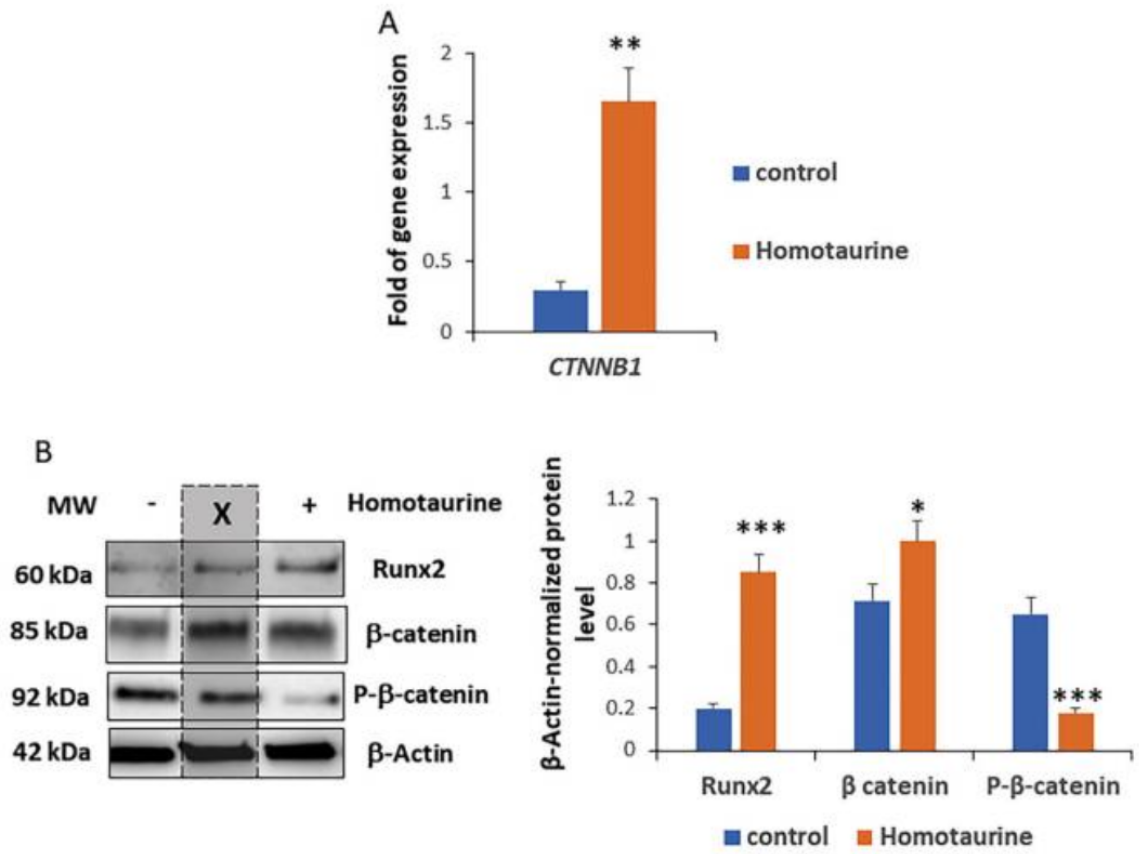

Figure 9: *Modulation of Wnt pathway by homotaurine treatment in LRRK2-G2019S mutated midbrain organoids. (A) Increased levels in CTNNB1 gene expression after homotaurine treatment. (B) Organoids treated with homotaurine revealed an increase in RUNX2 and β-catenin protein levels and a decrease in P-β-catenin levels. (*p<0.05;**p<0.01;***p<0.005).*

4.4 Impact of Glutathione on Mesenchymal Stem Cell Viability and ROS Levels

To determine the protective role of GSH on MSCs, we performed CCK-8 assay and DCDFA assay. Treatment with GSH not only enhanced the viability of MSCs but also preserved cell viability under oxidative stress conditions (Figure 10A).

When cells were exposed to hydrogen peroxide (H_2O_2) or tert-butyl hydroperoxide (TBHP), GSH significantly reduced the cytotoxic effects typically associated with these agents (Figure 10B). This protective action was confirmed by a decrease in intracellular ROS accumulation (Figure 10C), suggesting that GSH acts both as a direct antioxidant and as a modulator of redox homeostasis, contributing to improved cell survival and functional stability under stress.

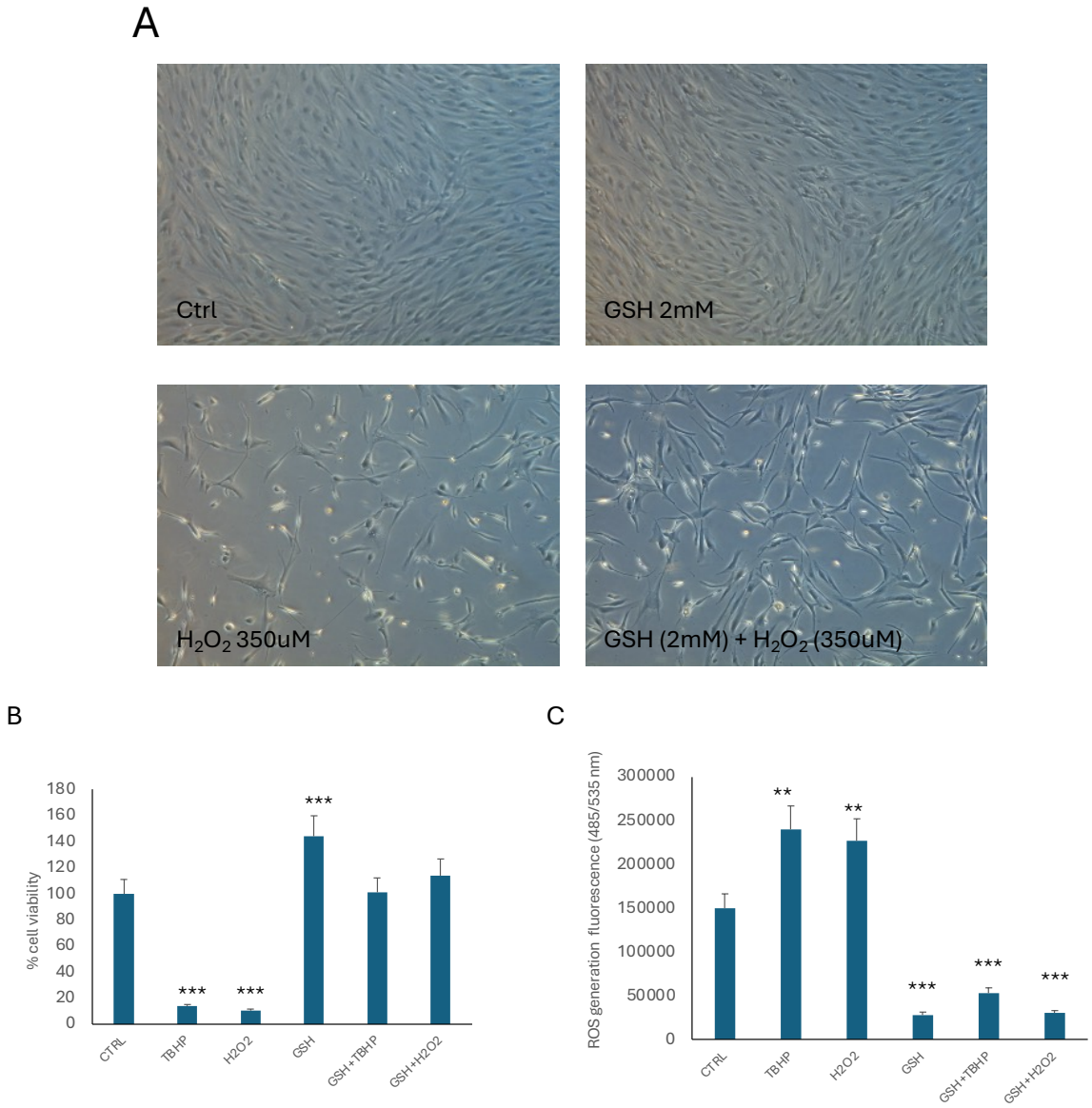

Figure 10: *Effects of GSH on MSCs morphology, viability and ROS levels. (A) Images of MSCs: top left untreated cells, top right cells treated with GSH, bottom left cells treated with H_2O_2, bottom right MSCs co-treated with GSH and H_2O_2. (B) Cell viability assay shows a reduction in viability in MSCs treated with TBHP and H_2O_2, while co-treatment with GSH restores viability to CTRL levels. (C) Intracellular ROS levels decrease in cells treated with GSH alone and are also reduced in the presence of H_2O_2 or TBHP when GSH is added. (**p<0.01;***p<0.005).*

4.5 Glutathione Prevents Stress-Induced Autophagy and Senescence, Protecting Mesenchymal Stem Cells

When cells are subjected to stress stimuli, such as H_2O_2, there is a clear activation of autophagy (Figure 11A), evidenced by increased levels of LC3B and a concomitant decrease in p62 expression. However, autophagy was inactive when cells were treated with GSH and H_2O_2, in fact p62 and LC3B levels were similar to those seen under control.

Senescence-related protein expression followed a similar pattern: stress induction proteins p53, SESN 2, and p21 levels, were high in cells stressed by H_2O_2 while cells treated with GSH alone or in combination with hydrogen peroxide maintained protein levels comparable to the control, adding to the evidence supporting GSH's anti-senescent and protective properties (Figure 11B).

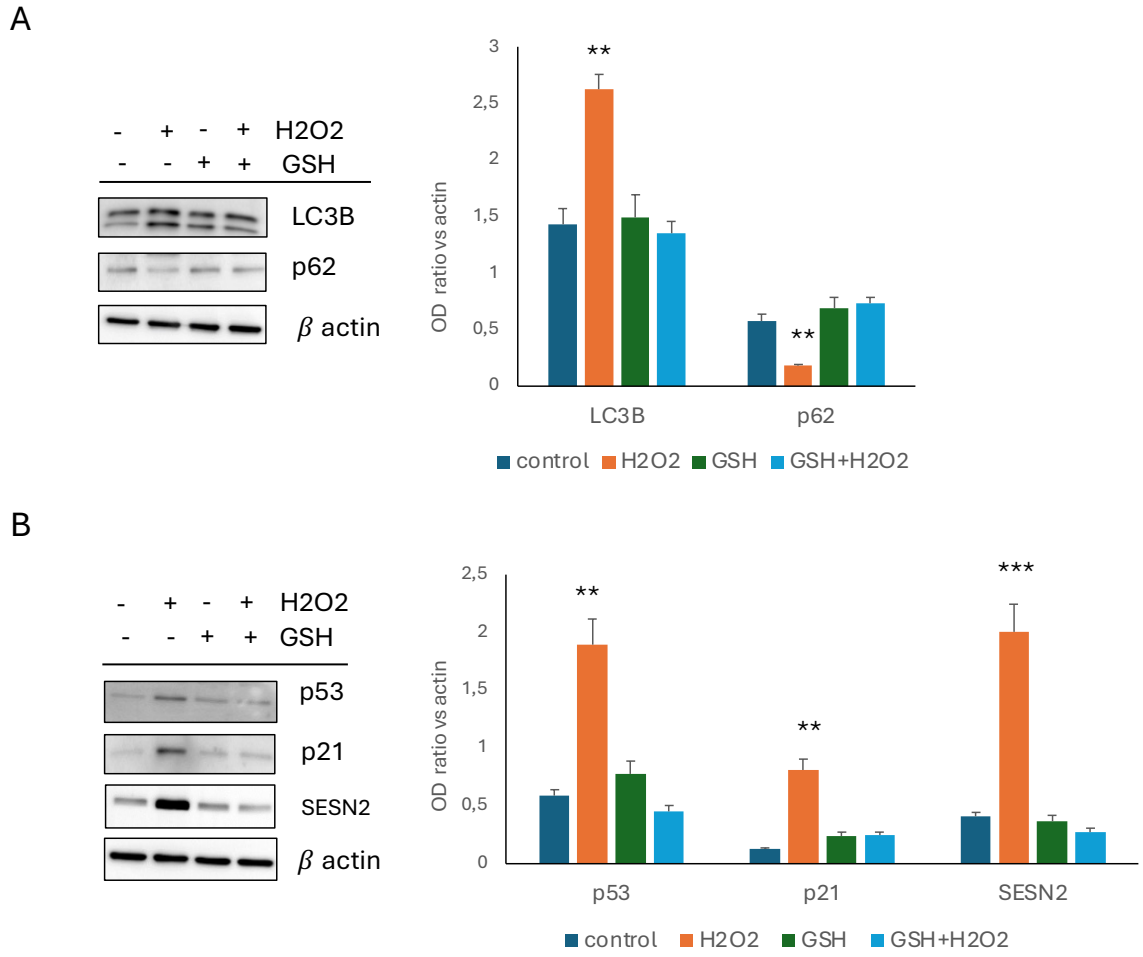

Figure 11: *GSH protects MSC from H_2O_2- Induced Autophagy and cellular stress. (A) H_2O_2 activates autophagy in MSCs, as indicated by increased LC3B and decreased p62 levels, while GSH co-treatment prevents these changes. (B) MSCs treated with H_2O_2 show elevated levels of p53, p21 and SESN2, whereas co-treated cells display levels comparable to CTRL.*
*(**p<0.01;***p<0.005).*

4.6 Protective Effects of GSH on Cell Viability and Oxidative Stress in Neuroblastoma Cells

When SH-SY5Y cells were exposed to TBHP or H_2O_2, a significant decrease in viability was observed (Figure 12A), indicating substantial oxidative damage. However, co-treatment with GSH effectively counteracts this effect, maintaining viability at levels comparable to

untreated control cells (Figure 12A). ROS assay followed the same trend as CCK-8 assay, cells treated with GSH in presence of TBHP or H_2O_2 showed ROS levels comparable to CTRL (Figure 12B). These results highlight the antioxidant capacity of GSH and its crucial role in protecting neuroblastoma cells from oxidative stress–induced cytotoxicity.

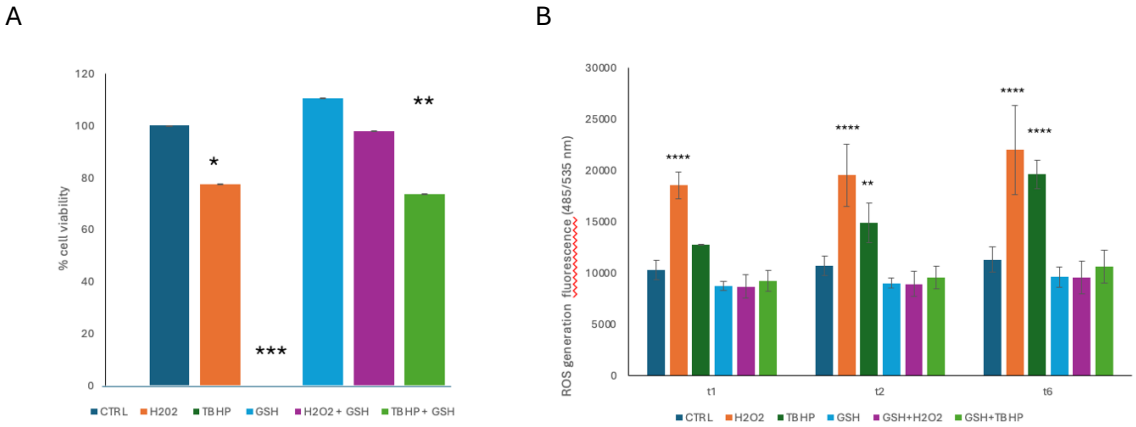

Figure 12: *Protective effects of GSH on SH-SY5Y cells. (A) GSH preserves cell viability in the presence of TBHP and H_2O_2. (B) GSH treatment reduces intracellular ROS levels, counteracting oxidative stress induced by H_2O_2. t1 ,t2, t6 indicate time points 1,2 and 6 hours after treatments respectively. (*p<0.05;**p<0.01;***p<0.005; ****p<0.0001).*

4.7 Characterization of Extracellular Vesicles Isolated from MSC Treated or Not with GSH

Extracellular vesicles (EVs) were separated from the conditioned medium of mesenchymal stem cells treated with GSH or not. EVs were quantified using Nanoparticle Tracking Analysis (NTA), which revealed that EVs from GSH-treated cells were significantly more abundant and had a slightly larger average diameter compared to those from untreated cells (Figure 13A). Characterization using the MACSPlex Exosome Kit revealed that both EV populations expressed the three classical tetraspanin markers (CD9, CD63, and CD81) (Figure 13B). Additionally, transmission electron microscopy (TEM) imaging confirmed the vesicles, revealing their characteristic spherical shape and size typical of extracellular vesicles (Figure 13C).

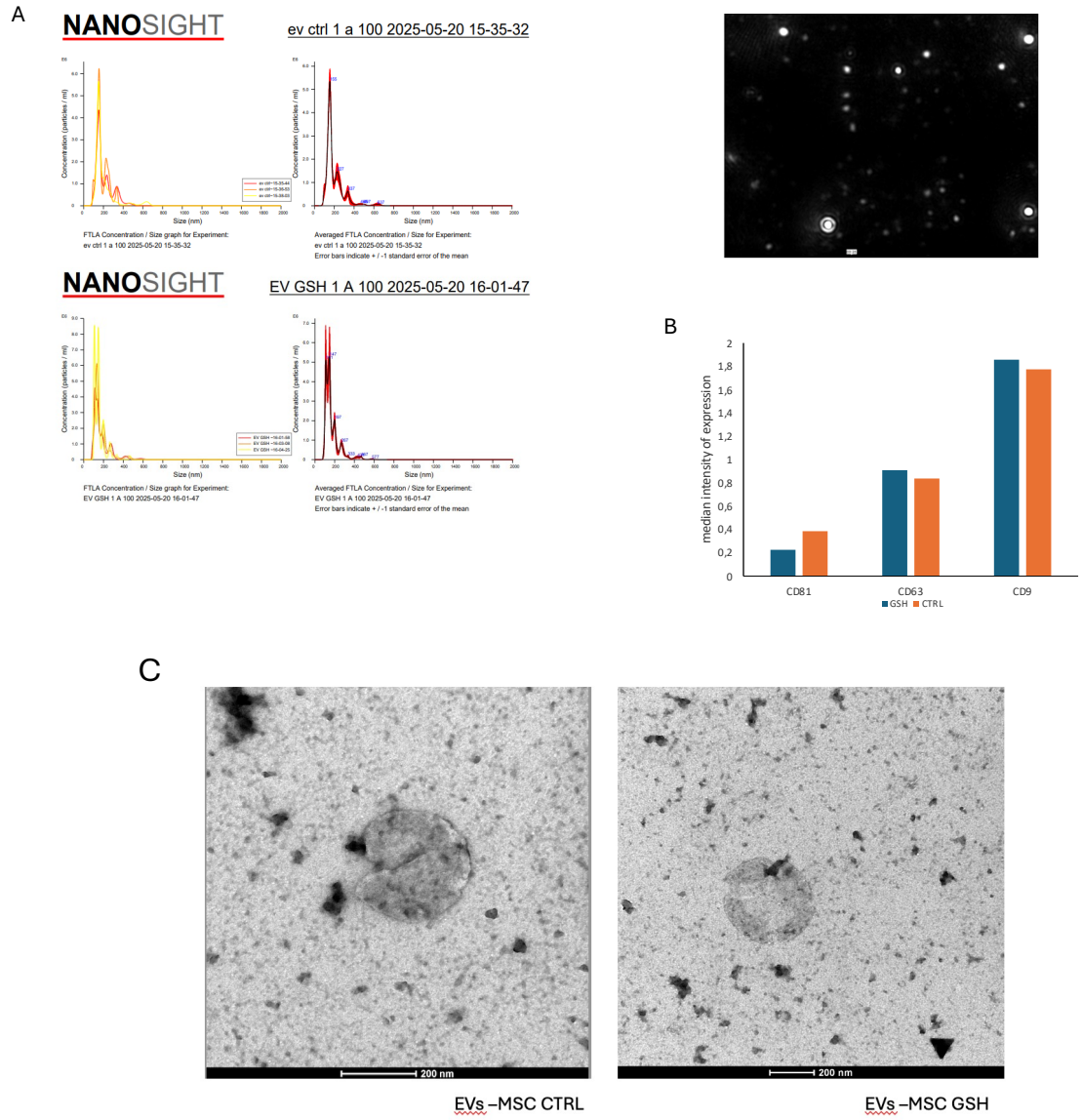

Figure 13: *Characterization of MSCs-EVs. (A) NTA plot showing the size distribution and concentration of EVs. The top-right figure shows EVs visualized by NTA. (B) Expression profile of EV-associated tetraspanins. (C) TEM images showing the typical morphology of EVs.*

4.8 Enhanced Protective Effects of GSH-EVs on Neuroblastoma Cells

EVs released by MSCs exerted a notable protective effect on SH-SY5Y, particularly under oxidative stress induced by H_2O_2. In fact, compared to EVs derived from untreated cells, EVs from GSH-treated MSCs showed a markedly stronger protective effect on stressed neuroblastoma cells, resulting in higher cell viability (Figure 14B) and a significant reduction in ROS levels (Figure 14C). These findings indicate that GSH treatment enhances the antioxidant and cytoprotective properties of mesenchymal stem cell–derived EVs,

reinforcing their potential role as carriers of protective bioactive molecules under oxidative stress conditions.

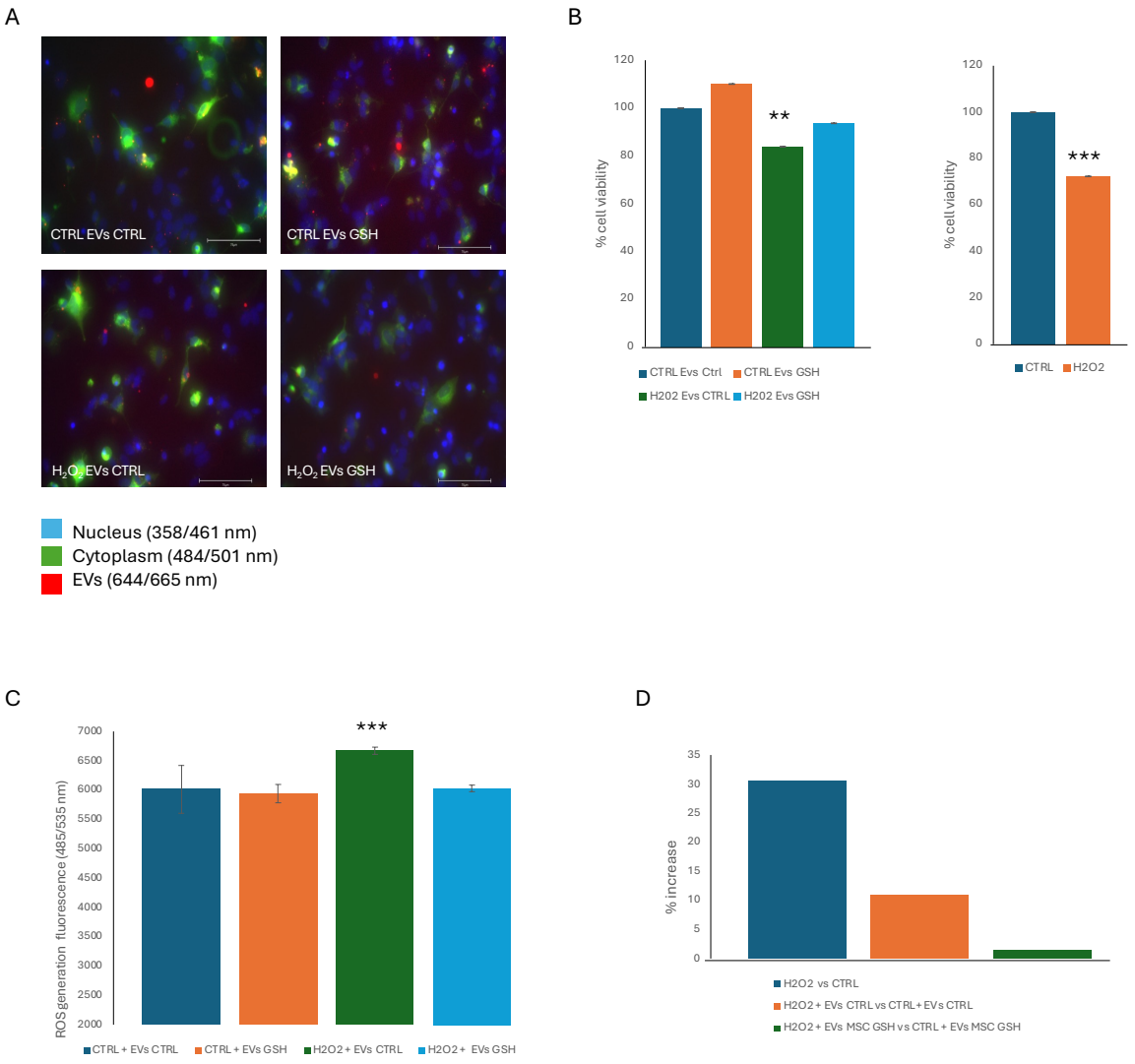

Figure 14: *Protective effect of GSH-EVs on SH-SY5Y. (A) EVs internalized in SH-SY5Y after 18h of incubation. (B) SH-SY5Y treated with GSH-EVs in the presence of H_2O_2 maintain viability comparable to CTRL, unlike cells treated with CTRL-EVs which show reduced viability. (C) ROS levels increase when cells are treated with CTRL-EVS. (D) H_2O_2 treatment induced a 30% increase in ROS, whereas the addition of GSH-EVs markedly reduces this rise, limiting the increase to about 1% (**p<0.01;***p<0.005).*

5. DISCUSSION

Aging and cellular senescence are closely related processes that lead to the gradual loss of tissue homeostasis and regenerative capacity. In many mammalian tissues, it has been demonstrated that the number of cells with senescent characteristics rises with age. Additionally, the buildup of senescent cells is linked to age-related tissue diseases like liver cirrhosis, atherosclerosis and osteoarthritis (Pawlikowski et al., 2013). The aim of this work was to investigate how homotaurine and glutathione confer protection and modulate the aging process. Following homotaurine treatment, MSCs showed increased cell viability and a significant decrease in intracellular ROS levels, confirming its protective role. In particular, these results showed that ROS levels in MSCs increased after 3 days of culture. This is in line with the literature, which reports that MSCs have a less efficient antioxidant defense system compared to other cell types (Denu & Hematti, 2016). It's known that elevated ROS levels induce oxidative stress causing cellular damage. The observed increase in ROS suggests that aging MSCs may experience significant oxidative stress, potentially impairing their regenerative capacity.

In this study MSCs treated with homotaurine showed a significant reduction in ROS levels, particularly after 14 days of treatment, whereas untreated MSCs displayed elevated ROS levels. Notably, this decrease in oxidative stress was accompanied by an increase in cell viability.

By reducing ROS levels and improving cell viability, homotaurine may mitigate the detrimental effects of oxidative stress and support the preservation of MSCs function during the aging. Homotaurine's potential as a therapeutic agent to mitigate the aging of stem cells is further supported by the long-lasting beneficial effects on cell viability that have been observed for up to 21 days. Sestrins are a group of proteins essential for preserving cellular homeostasis and controlling stress reactions, especially when oxidative stress is present (S.-D. Chen et al., 2019; Dalina et al., 2018). Following homotaurine treatment, Sestrin 1 levels significantly increased, suggesting that homotaurine may improve the cellular stress response by triggering the defenses against oxidative damage. We did not observe alterations in the expression of Sestrin 2, probably because homotaurine may have a selective effect on the Sestrin family, underscoring its potential to regulate a particular stress response pathway. Additionally, the reduction in p21 levels following homotaurine treatment suggests that it may modulate the cell cycle, potentially improving cell function and survival. Instead of inducing the typical DNA damage response, homotaurine may enhance cellular resilience

through alternative pathways, as indicated by the unaltered p53 levels. These findings support the hypothesis that, rather than widely activating the cellular damage response, the benefits of homotaurine in aging MSCs may result from the selective regulation of stress-related pathways, such as Sestrin 1 and p21.

MSCs are known to play a key role in supporting skeletal regeneration, contributing to bone formation, remodeling and repair (Pittenger et al., 2019). Given the beneficial effects of homotaurine observed in MSCs, the attention was moved to understand if the effect could be extended to the skeletal level using the zebrafish (Danio rerio) as a model organism. In this study we observed a significant increase in the expression of osteogenic markers like ctnnb1, Runx2b, and Sp7 in both zebrafish larvae and 4-month old (adult) zebrafish. These results suggest that homotaurine may promote skeletal health and regeneration, which is in line with the genes' known function in controlling bone formation.

Furthermore, the increase in VEGFR2 expression observed in 36-month old zebrafish following homotaurine treatment raises the possibility that homotaurine may enhance angiogenesis, which is frequently compromised with aging. This could improve overall tissue health and regeneration in aging models. These findings highlight the wide range of regenerative benefits of homotaurine, which go beyond stem cell activity to support osteogenesis and angiogenesis.

The definition of Parkinson's disease (PD) has gradually changed from a traditional akinetic-rigid movement disorder to a complex multi-system neurodegenerative disease that affects several cognitive domains and has crippling effects on patients (Mak et al., 2015). According to recent molecular, biological, and genetic research, the PD risk genes are expressed not only in the brain but also in peripheral organs and tissues, such as bone cells.

Because of their reduced mobility, postural instability, neurological impairment and decreased bone mass, people with PD are more likely to experience bone and joint issues and fractures, which are thought to be caused by falls (Xiong et al., 2021). Moreover, is known that LRRK2-G2019S cause the dysregulation of essential signaling pathway such as Wnt/β-catenin, which is important for neuroprotection, differentiation and bone homeostasis, or Runx2 the master gene of osteogenic differentiation. Recent studies highlight that homotaurine is able to interacts with Wnt/β-catenin. To study the effect of homotaurine in a PD model were used 3D neural epithelial stem cell (NESC) organoids derived from iPSCs carrying the LRRK2-G2019S mutation. In this research homotaurine treatment not only restored β-catenin expression in organoids but also increased the levels of Runx2. Thus, our findings suggest a shared pathological mechanism that homotaurine

may help mitigate. By modulating the expression of both Runx2 and β-catenin, homotaurine demonstrates a broad therapeutic potential. The ability of homotaurine to restore the function of the Wnt/β-catenin pathway is a dual therapeutic approach, as it is essential for both neuronal and skeletal health. This is especially important when it comes to treating the elevated risk of fractures and the related morbidity in Parkinson's disease patients. Furthermore, organoids treated with homotaurine showed a decrease in ROS levels, this result suggest that its protective effect can be linked to reduce oxidative stress, that is typical in PD.

It is evident that the accumulation of ROS is a key characteristic of many harmful molecular pathways that are present in early-stage PD, before neuron death begins. Excessive ROS accumulation can accelerate or directly trigger numerous cell death pathways, such as intrinsic and extrinsic apoptosis, cytoplasmic cell death and autophagic cell death (Trist et al., 2019). Among the cellular defense mechanism against oxidative stress, GSH is the most abundant non-protein thiol. It plays a central role in maintaining redox homeostasis and modulating key biological processes such as cell proliferation, apoptosis, immune response and fibrogenesis. Furthermore, GSH is a major determinant of redox signaling and is essential for xenobiotic detoxification (Lu, 2013). Post-mortem analyses of the central nervous system of PD patients have consistently shown significantly reduced GSH levels in the substantia nigra compared to age-matched controls, while no comparable reduction has been observed in other brain regions(Smeyne & Smeyne, 2013). This selective depletion of GSH suggests a region-specific vulnerability that may contribute to the oxidative stress and neuronal degeneration characteristic of PD. Accordingly, exploring treatments that enhance GSH-mediated antioxidant capacity is a logical approach. Through paracrine signaling, MSCs display neuroprotective qualities. Depending on the surrounding microenvironment, they can either strengthen or drive the inflammatory response toward resolution. According to earlier research, MSCs can significantly alter the neurodegenerative microenvironments associated with PD by inhibiting apoptosis, increasing neurogenesis and neuronal differentiation, improving autophagy, and modulating neuroinflammation and α-syn propagation (Shin et al., 2022). GSH has been shown to have a protective effect in MSC when hydrogen H_2O_2 treatment caused oxidative stress. We observed that cell viability was significantly reduced by H_2O_2 exposure alone, but it was maintained at levels like the untreated control group upon the addition of GSH. GSH's ability to mitigate oxidative stress in these cells was further supported by measurements of ROS production, which was significantly lower after GSH supplementation but significantly higher after H_2O_2 treatment.

An accumulation of ROS causes molecular damage and activates pathways that support cellular adaptability and survival, an example is autophagy. In this study, treatment with H_2O_2 induced autophagy activation with an increase in LC3B levels and a decrease in p62 levels. These results are in line with the canonical interpretation of increased autophagic activity (Bresciani et al., 2018). On the other hand, MSCs didn't activate autophagy when they were co-treated both with H_2O_2 and GSH. In particular, p62 and LC3B didn't exhibit the same modulation as in the H_2O_2 condition. According with these results, GSH is probably protective against oxidative stress.

In addition to the autophagy related changes, key stress-response proteins were also investigated. In our study, H_2O_2 treatment caused a marked increase in p53, p21, and SESN2 levels, consistent with their roles as stress-responsive genes. In contrast, MSCs treated with H_2O_2 in combination with GSH did not show this upregulation, confirming GSH's ability to maintain redox homeostasis and prevent activation of stress pathways. Due to its high oxygen consumption and abundance of redox active metals, the brain is especially vulnerable to oxidative stress (Wang, 2010). In PD, oxidative stress plays a central role in the degeneration of dopaminergic neurons (Dias et al., 2013), and one possible contributing factor is the marked decrease in intracellular GSH levels observed in the substantia nigra (Wang, 2010). The SH-SY5Y used as in vitro neuronal model exhibit many characteristics of dopaminergic neurons making them a good model for PD research (Xie et al., 2010). GSH exerts significant protective effects on SH-SY5Y by enhancing their resistance to oxidative stress and preserving cell viability. In our study, we observed that the cytotoxic effect of H_2O_2 was completely abolished by GSH treatment, thereby preserving cell viability. Similarly, intracellular ROS levels were significantly reduced in presence of the GSH. Thus, in this work, GSH clearly demonstrate its protective role in *vitro* in both cellular models used (MSCs and SH-SY5Y) counteracting oxidative damage and preserving cell viability. However, the therapeutic use of GSH *in vivo* faced several limitations. When administered orally, GSH exhibits a short half-life and doesn't lead to significant increase in systemic GSH levels, highlighting its poor bioavailability (Allen & Bradley, 2011). To overcome this limitation, the encapsulation of GSH into lipid-based carriers, such as liposomes, has been proposed to enhance its absorption efficiency and cellular uptake (Sinha et al., 2018). Extracellular vesicles (EVs) have emerged as highly promising cell-free therapeutic strategy because of their ability to naturally transport signaling molecules, like proteins, lipids and microRNA (Wang & Pan, 2023). MSC-derived EVs, in particular, display a notable anti-inflammatory and cytoprotective effects, reflecting the function of their parent cells (Abreu

et al., 2016). This makes them ideal candidates for delivering therapeutic molecules. In this context, we explored the potential of MSC-EVs as natural GSH carriers, potentially enhancing their intrinsic protective activity and providing a more efficient way to supply GSH to target cells. Treatment with GSH-EVs maintained cell viability at stable levels. While H_2O_2 alone increased ROS levels by approximately 30% compared to controls, treatment with CTRL-EVs limited this rise to a 10%. Remarkably, GSH-EVs almost completely prevented ROS accumulation, resulting in only a 1% increase and effectively maintaining ROS levels to those of untreated cells.

These results suggest that GSH-EVs could serve as a highly effective cell-free strategy to deliver antioxidant protection in oxidative stress conditions.

6. CONCLUSIONS

Aging is a gradually loss of physiological integrity, which contributes to the onset of disease like osteoporosis and neurodegenerative disorders. One of the main factors driving this decline is oxidative stress. This aimed to investigate the effects of homotaurine and GSH on oxidative stress and their protective roles in age-related diseases. Both molecules demonstrated protective effects on MSCs viability and oxidative stress, which is particularly important given the central role of MSCs in bone regeneration and tissue homeostasis.

In this study we also demonstrated that the protective effect of GSH is propagated at paracrine level: EVs isolated from GSH-pretreated MSC were able to preserve cell viability and counteract oxidative damage on SH-SY5Y opening new perspectives in regenerative medicine, where EVs are emerging as innovative cell-free therapeutic tools.

Overall, these findings suggest that homotaurine and GSH may serve as valuable molecules for combating oxidative stress-driven aging and its associated pathologies. This study has extended our knowledge of the advantageous effect of homotaurine and GSH, highlighting their potential as therapeutic candidates for the prevention of aging-related diseases, such as neurodegenerative and skeletal disorders. Nonetheless, further studies are required to understand the specific molecular mechanisms underlying the protective effects of GSH-EVs, optimizing EV loading strategies and testing their therapeutic efficacy in *in vivo* models of neurodegenerative and skeletal diseases. In addition, investigating the safety of EV-based therapies will be essential to support their potential clinical translation.

7. REFERENCES

Abreu, S. C., Weiss, D. J., & Rocco, P. R. M. (2016). Extracellular vesicles derived from mesenchymal stromal cells: a therapeutic option in respiratory diseases? *Stem Cell Research & Therapy*, *7*(1), 53. https://doi.org/10.1186/s13287-016-0317-0

Ahmad, A. M., Mohammed, H. A., Faris, T. M., Hassan, A. S., Mohamed, H. B., El Dosoky, M. I., & Aboubakr, E. M. (2021). Nano-Structured Lipid Carrier-Based Oral Glutathione Formulation Mediates Renoprotection against Cyclophosphamide-Induced Nephrotoxicity, and Improves Oral Bioavailability of Glutathione Confirmed through RP-HPLC Micellar Liquid Chromatography. *Molecules*, *26*(24), 7491. https://doi.org/10.3390/molecules26247491

Allen, J., & Bradley, R. D. (2011). Effects of Oral Glutathione Supplementation on Systemic Oxidative Stress Biomarkers in Human Volunteers. *The Journal of Alternative and Complementary Medicine*, *17*(9), 827–833. https://doi.org/10.1089/acm.2010.0716

Andonian, B. J., Hippensteel, J. A., Abuabara, K., Boyle, E. M., Colbert, J. F., Devinney, M. J., Faye, A. S., Kochar, B., Lee, J., Litke, R., Nair, D., Sattui, S. E., Sheshadri, A., Sherman, A. N., Singh, N., Zhang, Y., & LaHue, S. C. (2024). Inflammation and aging-related disease: A transdisciplinary inflammaging framework. *GeroScience*, *47*(1), 515–542. https://doi.org/10.1007/s11357-024-01364-0

Alzheimer's Association. (2019). Alzheimer's disease facts and figures. *Alzheimer's & Dementia: The Journal of the Alzheimer's Association, 15*(3), 321–387. https://doi.org/10.1016/j.jalz.2019.01.010

Averill-Bates, D. (2024). Reactive oxygen species and cell signaling. Review. *Biochimica et Biophysica Acta (BBA) - Molecular Cell Research*, *1871*(2), 119573. https://doi.org/10.1016/j.bbamcr.2023.119573

Bossù, P., Salani, F., Ciaramella, A., Sacchinelli, E., Mosca, A., Banaj, N., Assogna, F., Orfei, M. D., Caltagirone, C., Gianni, W., & Spalletta, G. (2018). Anti-inflammatory Effects of Homotaurine in Patients With Amnestic Mild Cognitive Impairment. *Frontiers in Aging Neuroscience*, *10*. https://doi.org/10.3389/fnagi.2018.00285

Bresciani, A., Spiezia, M. C., Boggio, R., Cariulo, C., Nordheim, A., Altobelli, R., Kuhlbrodt, K., Dominguez, C., Munoz-Sanjuan, I., Wityak, J., Fodale, V., Marchionini, D. M., & Weiss, A. (2018). Quantifying autophagy using novel LC3B and p62 TR-FRET assays. *PLOS ONE*, *13*(3), e0194423. https://doi.org/10.1371/journal.pone.0194423

Budanov, A. V., & Karin, M. (2008). p53 Target Genes Sestrin1 and Sestrin2 Connect Genotoxic Stress and mTOR Signaling. *Cell*, *134*(3), 451–460. https://doi.org/10.1016/j.cell.2008.06.028

Campisi, J., & d'Adda di Fagagna, F. (2007). Cellular senescence: when bad things happen to good cells. *Nature Reviews Molecular Cell Biology*, *8*(9), 729–740. https://doi.org/10.1038/nrm2233

Chen, P.-M., Lin, C.-H., Li, N.-T., Wu, Y.-M., Lin, M.-T., Hung, S.-C., & Yen, M.-L. (2015). c-Maf regulates pluripotency genes, proliferation/self-renewal, and lineage commitment in ROS-mediated senescence of human mesenchymal stem cells. *Oncotarget*, *6*(34), 35404–35418. https://doi.org/10.18632/oncotarget.6178

Chen, S.-D., Yang, J.-L., Lin, T.-K., & Yang, D.-I. (2019). Emerging Roles of Sestrins in Neurodegenerative Diseases: Counteracting Oxidative Stress and Beyond. *Journal of Clinical Medicine*, *8*(7), 1001. https://doi.org/10.3390/jcm8071001

Chen, Y., Yi, H., Liao, S., He, J., Zhou, Y., & Lei, Y. (2025). LC3B: A microtubule-associated protein influences disease progression and prognosis. *Cytokine & Growth Factor Reviews*, *81*, 16–26. https://doi.org/10.1016/j.cytogfr.2024.11.006

Childs, B. G., Durik, M., Baker, D. J., & van Deursen, J. M. (2015). Cellular senescence in aging and age-related disease: from mechanisms to therapy. *Nature Medicine*, *21*(12), 1424–1435. https://doi.org/10.1038/nm.4000

da Silva, P. F. L., & Schumacher, B. (2021). Principles of the Molecular and Cellular Mechanisms of Aging. *Journal of Investigative Dermatology*, *141*(4), 951–960. https://doi.org/10.1016/j.jid.2020.11.018

Dabrowska S, Andrzejewska A, Janowski M, Lukomska B. Immunomodulatory and Regenerative Effects of Mesenchymal Stem Cells and Extracellular Vesicles: Therapeutic Outlook for Inflammatory and Degenerative Diseases. *Front Immunol.* 2021 Feb 5;11:591065. doi: 10.3389/fimmu.2020.591065. PMID: 33613514; PMCID: PMC7893976.

Dalina, A. A., Kovaleva, I. E., & Budanov, A. V. (2018). Sestrins are Gatekeepers in the Way from Stress to Aging and Disease. *Molecular Biology*, *52*(6), 823–835. https://doi.org/10.1134/S0026893318060043

Davinelli, S., Chiosi, F., Di Marco, R., Costagliola, C., & Scapagnini, G. (2017). Cytoprotective Effects of Citicoline and Homotaurine against Glutamate and High Glucose Neurotoxicity in Primary Cultured Retinal Cells. *Oxidative Medicine and Cellular Longevity*, *2017*(1). https://doi.org/10.1155/2017/2825703

Denu, R. A., & Hematti, P. (2016). Effects of Oxidative Stress on Mesenchymal Stem Cell Biology. *Oxidative Medicine and Cellular Longevity*, *2016*(1). https://doi.org/10.1155/2016/2989076

Di Micco, R., Krizhanovsky, V., Baker, D., & d'Adda di Fagagna, F. (2021). Cellular senescence in ageing: from mechanisms to therapeutic opportunities. *Nature Reviews Molecular Cell Biology*, *22*(2), 75–95. https://doi.org/10.1038/s41580-020-00314-w

Dias, V., Junn, E., & Mouradian, M. M. (2013). The Role of Oxidative Stress in Parkinson's Disease. *Journal of Parkinson's Disease*, *3*(4), 461–491. https://doi.org/10.3233/JPD-130230

Farnebo, M., Bykov, V. J. N., & Wiman, K. G. (2010). The p53 tumor suppressor: A master regulator of diverse cellular processes and therapeutic target in cancer. *Biochemical and Biophysical Research Communications*, *396*(1), 85–89. https://doi.org/10.1016/j.bbrc.2010.02.152

Ferrucci, L., & Fabbri, E. (2018). Inflammageing: chronic inflammation in ageing, cardiovascular disease, and frailty. *Nature Reviews. Cardiology*, *15*(9), 505–522. https://doi.org/10.1038/s41569-018-0064-2

Gayatri Jayendran Nair, Yashwi Sinha, Ajeet Kumar Srivastava, Narendra S Kumar, & Lingayya Hiremath. (2023). A review on the molecular basis of stemness of mesenchymal stem cells. *World Journal of Biology Pharmacy and Health Sciences*, *15*(2), 202–207. https://doi.org/10.30574/wjbphs.2023.15.2.0362

Gildee Cristina. (2025). *Bone Functional Adaptation: Life History Constraints and Implications for Aging Research*.

Giordano, S., Darley-Usmar, V., & Zhang, J. (2014). Autophagy as an essential cellular antioxidant pathway in neurodegenerative disease. *Redox Biology*, *2*, 82–90. https://doi.org/10.1016/j.redox.2013.12.013

Goyal, A., Afzal, M., Khan, N. H., Goyal, K., Srinivasamurthy, S. K., Gupta, G., Benod Kumar, K., Ali, H., Rana, M., Wong, L. S., Kumarasamy, V., & Subramaniyan, V. (2025). Targeting p53-p21 signaling to enhance mesenchymal stem cell regenerative potential. *Regenerative Therapy*, *29*, 352–363. https://doi.org/10.1016/j.reth.2025.03.007

Guloyan, V., Oganesian, B., Baghdasaryan, N., Yeh, C., Singh, M., Guilford, F., Ting, Y.-S., & Venketaraman, V. (2020). Glutathione Supplementation as an Adjunctive Therapy in COVID-19. *Antioxidants*, *9*(10), 914. https://doi.org/10.3390/antiox9100914

Guo, Z., Wang, G., Wu, B., Chou, W.-C., Cheng, L., Zhou, C., Lou, J., Wu, D., Su, L., Zheng, J., Ting, J. P.-Y., & Wan, Y. Y. (2020). DCAF1 regulates Treg senescence via the ROS axis during immunological aging. *Journal of Clinical Investigation*, *130*(11), 5893–5908. https://doi.org/10.1172/JCI136466

Hajam, Y. A., Rani, R., Ganie, S. Y., Sheikh, T. A., Javaid, D., Qadri, S. S., Pramodh, S., Alsulimani, A., Alkhanani, M. F., Harakeh, S., Hussain, A., Haque, S., & Reshi, M. S. (2022). Oxidative Stress in Human Pathology and Aging: Molecular Mechanisms and Perspectives. *Cells*, *11*(3), 552. https://doi.org/10.3390/cells11030552

Han, J., Wu, J., & Silke, J. (2020). An overview of mammalian p38 mitogen-activated protein kinases, central regulators of cell stress and receptor signaling. *F1000Research*, *9*, 653. https://doi.org/10.12688/f1000research.22092.1

Jena, A. B., Samal, R. R., Bhol, N. K., & Duttaroy, A. K. (2023). Cellular Red-Ox system in health and disease: The latest update. *Biomedicine & Pharmacotherapy*, *162*, 114606. https://doi.org/10.1016/j.biopha.2023.114606

Jesuthasan, A., Magrinelli, F., Batla, A., & Bhatia, K. P. (2025). Rare Movement Disorders—An Approach for Clinicians. *International Journal of Molecular Sciences*, *26*(13), 6024. https://doi.org/10.3390/ijms26136024

Jovic, D., Yu, Y., Wang, D., Wang, K., Li, H., Xu, F., Liu, C., Liu, J., & Luo, Y. (2022). A Brief Overview of Global Trends in MSC-Based Cell Therapy. *Stem Cell Reviews and Reports*, *18*(5), 1525–1545. https://doi.org/10.1007/s12015-022-10369-1

Juan, C. A., Pérez de la Lastra, J. M., Plou, F. J., & Pérez-Lebeña, E. (2021). The Chemistry of Reactive Oxygen Species (ROS) Revisited: Outlining Their Role in Biological Macromolecules (DNA, Lipids and Proteins) and Induced Pathologies. *International Journal of Molecular Sciences*, *22*(9), 4642. https://doi.org/10.3390/ijms22094642

Kalamkar, S., Acharya, J., Kolappurath Madathil, A., Gajjar, V., Divate, U., Karandikar-Iyer, S., Goel, P., & Ghaskadbi, S. (2022). Randomized Clinical Trial of How Long-Term Glutathione Supplementation Offers Protection from Oxidative Damage and Improves HbA1c in Elderly Type 2 Diabetic Patients. *Antioxidants*, *11*(5), 1026. https://doi.org/10.3390/antiox11051026

Kirtonia, A., Sethi, G., & Garg, M. (2020). The multifaceted role of reactive oxygen species in tumorigenesis. *Cellular and Molecular Life Sciences*, *77*(22), 4459–4483. https://doi.org/10.1007/s00018-020-03536-5

Kvistad, C. E., Kråkenes, T., Gjerde, C., Mustafa, K., Rekand, T., & Bø, L. (2022). Safety and Clinical Efficacy of Mesenchymal Stem Cell Treatment in Traumatic Spinal Cord

Injury, Multiple Sclerosis and Ischemic Stroke – A Systematic Review and Meta-Analysis. *Frontiers in Neurology*, *13*. https://doi.org/10.3389/fneur.2022.891514

Lawrence, M., Goyal, A., Pathak, S., & Ganguly, P. (2024). Cellular Senescence and Inflammaging in the Bone: Pathways, Genetics, Anti-Aging Strategies and Interventions. *International Journal of Molecular Sciences*, *25*(13), 7411. https://doi.org/10.3390/ijms25137411

Lee, J. H., Won, Y. J., Kim, H., Choi, M., Lee, E., Ryoou, B., Lee, S.-G., & Cho, B. S. (2023). Adipose Tissue-Derived Mesenchymal Stem Cell-Derived Exosomes Promote Wound Healing and Tissue Regeneration. *International Journal of Molecular Sciences*, *24*(13), 10434. https://doi.org/10.3390/ijms241310434

Li, H., Xia, S., Xu, S., Liu, P., Gu, Y., Bao, X., Xu, Y., & Cao, X. (2021). γ-Glutamylcysteine Alleviates Ischemic Stroke-Induced Neuronal Apoptosis by Inhibiting ROS-Mediated Endoplasmic Reticulum Stress. *Oxidative Medicine and Cellular Longevity*, *2021*(1). https://doi.org/10.1155/2021/2961079

Li, L., Tan, J., Miao, Y., Lei, P., & Zhang, Q. (2015). ROS and Autophagy: Interactions and Molecular Regulatory Mechanisms. *Cellular and Molecular Neurobiology*, *35*(5), 615–621. https://doi.org/10.1007/s10571-015-0166-x

Liu, W. J., Ye, L., Huang, W. F., Guo, L. J., Xu, Z. G., Wu, H. L., Yang, C., & Liu, H. F. (2016). p62 links the autophagy pathway and the ubiqutin–proteasome system upon ubiquitinated protein degradation. *Cellular & Molecular Biology Letters*, *21*(1), 29. https://doi.org/10.1186/s11658-016-0031-z

López-Otín, C., Blasco, M. A., Partridge, L., Serrano, M., & Kroemer, G. (2023). Hallmarks of aging: An expanding universe. *Cell*, *186*(2), 243–278. https://doi.org/10.1016/j.cell.2022.11.001

Lu, S. C. (2013). Glutathione synthesis. *Biochimica et Biophysica Acta (BBA) - General Subjects*, *1830*(5), 3143–3153. https://doi.org/10.1016/j.bbagen.2012.09.008

Lyons, C. E., Pallais, J. P., McGonigle, S., Mansk, R. P., Collinge, C. W., Yousefzadeh, M. J., Baker, D. J., Schrank, P. R., Williams, J. W., Niedernhofer, L. J., van Deursen, J. M., Razzoli, M., & Bartolomucci, A. (2024). Chronic social stress induces p16-mediated senescent cell accumulation in mice. *Nature Aging*, *5*(1), 48–64. https://doi.org/10.1038/s43587-024-00743-8

Lyons, C. E., Pallais, J. P., McGonigle, S., Mansk, R. P., Collinge, C. W., Yousefzadeh, M. J., Baker, D. J., Schrank, P. R., Williams, J. W., Niedernhofer, L. J., van Deursen, J. M., Razzoli, M., & Bartolomucci, A. (2025). Chronic social stress induces p16-

mediated senescent cell accumulation in mice. *Nature Aging*, *5*(1), 48–64. https://doi.org/10.1038/s43587-024-00743-8

Madathil, A. K., Ghaskadbi, S., Kalamkar, S., & Goel, P. (2023). Pune GSH supplementation study: Analyzing longitudinal changes in type 2 diabetic patients using linear mixed-effects models. *Frontiers in Pharmacology*, *14*. https://doi.org/10.3389/fphar.2023.1139673

Mak, E., Su, L., Williams, G. B., Firbank, M. J., Lawson, R. A., Yarnall, A. J., Duncan, G. W., Owen, A. M., Khoo, T. K., Brooks, D. J., Rowe, J. B., Barker, R. A., Burn, D. J., & O'Brien, J. T. (2015). Baseline and longitudinal grey matter changes in newly diagnosed Parkinson's disease: ICICLE-PD study. *Brain*, *138*(10), 2974–2986. https://doi.org/10.1093/brain/awv211

Minich, D. M., & Brown, B. I. (2019). A Review of Dietary (Phyto)Nutrients for Glutathione Support. *Nutrients*, *11*(9), 2073. https://doi.org/10.3390/nu11092073

Minoia, A., Piritore, F. C., Bolognin, S., Pessoa, J., Bernardes de Jesus, B., Tiso, N., Romanelli, M. G., Schwamborn, J. C., Dalle Carbonare, L., & Valenti, M. T. (2025). Antioxidant, Osteogenic, and Neuroprotective Effects of Homotaurine in Aging and Parkinson's Disease Models. *Antioxidants*, *14*(3), 249. https://doi.org/10.3390/antiox14030249

Mulcahy, L. A., Pink, R. C., & Carter, D. R. F. (2014). Routes and mechanisms of extracellular vesicle uptake. *Journal of Extracellular Vesicles*, *3*(1). https://doi.org/10.3402/jev.v3.24641

Mushahary, D., Spittler, A., Kasper, C., Weber, V., & Charwat, V. (2018). Isolation, cultivation, and characterization of human mesenchymal stem cells. *Cytometry Part A*, *93*(1), 19–31. https://doi.org/10.1002/cyto.a.23242

Nieto-Estevez, V., Changarathil, G., Adeyeye, A. O., Coppin, M. O., Kassim, R. S., Zhu, J., & Hsieh, J. (2022). HDAC1 Regulates Neuronal Differentiation. *Frontiers in Molecular Neuroscience*, *14*. https://doi.org/10.3389/fnmol.2021.815808

Noh, J. H., Kim, K. M., Idda, M. L., Martindale, J. L., Yang, X., Abdelmohsen, K., & Gorospe, M. (2018). GRSF1 suppresses cell senescence. *Aging*, *10*(8), 1856–1866. https://doi.org/10.18632/aging.101516

Oh, C., Koh, D., Jeon, H. Bin, & Kim, K. M. (2022). The Role of Extracellular Vesicles in Senescence. *Molecules and Cells*, *45*(9), 603–609. https://doi.org/10.14348/molcells.2022.0056

Ornatowski, W., Lu, Q., Yegambaram, M., Garcia, A. E., Zemskov, E. A., Maltepe, E., Fineman, J. R., Wang, T., & Black, S. M. (2020). Complex interplay between autophagy and oxidative stress in the development of pulmonary disease. *Redox Biology*, *36*, 101679. https://doi.org/10.1016/j.redox.2020.101679

Pandey, K. B. (2025). From bench to bedside: translational insights into aging research. *Frontiers in Aging*, *6*. https://doi.org/10.3389/fragi.2025.1492099

Pawlikowski, J. S., Adams, P. D., & Nelson, D. M. (2013). Senescence at a glance. *Journal of Cell Science*. https://doi.org/10.1242/jcs.109728

Pellegrino D, La Russa D, Marrone A. Oxidative Imbalance and Kidney Damage: New Study Perspectives from Animal Models to Hospitalized Patients. *Antioxidants (Basel).* 2019 Nov 28;8(12):594. doi: 10.3390/antiox8120594. PMID: 31795160; PMCID: PMC6943704.

Petrova, N. V., Velichko, A. K., Razin, S. V., & Kantidze, O. L. (2016). Small molecule compounds that induce cellular senescence. *Aging Cell*, *15*(6), 999–1017. https://doi.org/10.1111/acel.12518

Pezone, A., Olivieri, F., Napoli, M. V., Procopio, A., Avvedimento, E. V., & Gabrielli, A. (2023). Inflammation and DNA damage: cause, effect or both. *Nature Reviews Rheumatology*, *19*(4), 200–211. https://doi.org/10.1038/s41584-022-00905-1

Pittenger, M. F., Discher, D. E., Péault, B. M., Phinney, D. G., Hare, J. M., & Caplan, A. I. (2019). Mesenchymal stem cell perspective: cell biology to clinical progress. *Npj Regenerative Medicine*, *4*(1), 22. https://doi.org/10.1038/s41536-019-0083-6

Pruteanu, L. L., Bailey, D. S., Grădinaru, A. C., & Jäntschi, L. (2023). The Biochemistry and Effectiveness of Antioxidants in Food, Fruits, and Marine Algae. *Antioxidants*, *12*(4), 860. https://doi.org/10.3390/antiox12040860

Qin, Y., Guan, J., & Zhang, C. (2014). Mesenchymal stem cells: mechanisms and role in bone regeneration. *Postgraduate Medical Journal*, *90*(1069), 643–647. https://doi.org/10.1136/postgradmedj-2013-132387

Ragnoli, B., Chiazza, F., Tarsi, G., & Malerba, M. (2025). Biological pathways and mechanisms linking COPD and cardiovascular disease. *Therapeutic Advances in Chronic Disease*, *16*. https://doi.org/10.1177/20406223251314286

Sajjad, R., Arif, R., Shah, A. A., Manzoor, I., & Mustafa, G. (2018). Pathogenesis of Alzheimer's Disease: Role of Amyloid-beta and Hyperphosphorylated Tau Protein. *Indian Journal of Pharmaceutical Sciences*, *80*(4). https://doi.org/10.4172/pharmaceutical-sciences.1000397

Samsonraj, R. M., Raghunath, M., Nurcombe, V., Hui, J. H., van Wijnen, A. J., & Cool, S. M. (2017). Concise Review: Multifaceted Characterization of Human Mesenchymal Stem Cells for Use in Regenerative Medicine. *Stem Cells Translational Medicine*, *6*(12), 2173–2185. https://doi.org/10.1002/sctm.17-0129

Santacroce, G., Gentile, A., Soriano, S., Novelli, A., Lenti, M. V., & Di Sabatino, A. (2023). Glutathione: Pharmacological aspects and implications for clinical use in non-alcoholic fatty liver disease. *Frontiers in Medicine*, *10*. https://doi.org/10.3389/fmed.2023.1124275

Selçuk, E. (2025). Beyond the Fracture: Mortality Risk and Survival after Hip Fractures in the Elderly. In *Longevity and Geriatrics*. IntechOpen. https://doi.org/10.5772/intechopen.1010851

Sharma, M., Bellio, M. A., Benny, M., Kulandavelu, S., Chen, P., Janjindamai, C., Han, C., Chang, L., Sterling, S., Williams, K., Damianos, A., Batlahally, S., Kelly, K., Aguilar-Caballero, D., Zambrano, R., Chen, S., Huang, J., Wu, S., Hare, J. M., … Young, K. (2022). Mesenchymal Stem Cell-derived Extracellular Vesicles Prevent Experimental Bronchopulmonary Dysplasia Complicated By Pulmonary Hypertension. *Stem Cells Translational Medicine*, *11*(8), 828–840. https://doi.org/10.1093/stcltm/szac041

Sharma, V., Unjum Saqib, B. Z., & Aran, K. R. (2025). Leptin as a potential neuroprotective target in Parkinson's Disease: Exploring its role in Neuroinflammation, oxidative Stress, and dopaminergic neurodegeneration. *Neuroscience*, *572*, 134–144. https://doi.org/10.1016/j.neuroscience.2025.03.008

Sharpless, N. E., & Sherr, C. J. (2015). Forging a signature of in vivo senescence. *Nature Reviews Cancer*, *15*(7), 397–408. https://doi.org/10.1038/nrc3960

Shin, J. Y., Kim, D.-Y., Lee, J., Shin, Y. J., Kim, Y. S., & Lee, P. H. (2022). Priming mesenchymal stem cells with α-synuclein enhances neuroprotective properties through induction of autophagy in Parkinsonian models. *Stem Cell Research & Therapy*, *13*(1), 483. https://doi.org/10.1186/s13287-022-03139-w

Sinha, R., Sinha, I., Calcagnotto, A., Trushin, N., Haley, J. S., Schell, T. D., & Richie, J. P. (2018). Oral supplementation with liposomal glutathione elevates body stores of glutathione and markers of immune function. *European Journal of Clinical Nutrition*, *72*(1), 105–111. https://doi.org/10.1038/ejcn.2017.132

Smeyne, M., & Smeyne, R. J. (2013). Glutathione metabolism and Parkinson's disease. *Free Radical Biology and Medicine*, *62*, 13–25. https://doi.org/10.1016/j.freeradbiomed.2013.05.001

Song, M. J., Park, C., Kim, H., Han, S., Lee, S. H., Lee, D. H., & Chung, J. H. (2023). Carnitine acetyltransferase deficiency mediates mitochondrial dysfunction-induced cellular senescence in dermal fibroblasts. *Aging Cell*, *22*(11). https://doi.org/10.1111/acel.14000

Tabet, C. G., Pacheco, R. L., Martimbianco, A. L. C., Riera, R., Hernandez, A. J., Bueno, D. F., & Fernandes, T. L. (2024). Advanced therapy with mesenchymal stromal cells for knee osteoarthritis: Systematic review and meta-analysis of randomized controlled trials. *Journal of Orthopaedic Translation*, *48*, 176–189. https://doi.org/10.1016/j.jot.2024.07.012

Tian, J., Dang, H., Wallner, M. *et al.* Homotaurine, a safe blood-brain barrier permeable $GABA_A$-R-specific agonist, ameliorates disease in mouse models of multiple sclerosis. *Sci Rep* **8**, 16555 (2018). https://doi.org/10.1038/s41598-018-32733-3

Toppi, E., Sireno, L., Lembo, M., Banaj, N., Messina, B., Golesorkhtafti, S., Spalletta, G., & Bossù, P. (2022). IL-33 and IL-10 Serum Levels Increase in MCI Patients Following Homotaurine Treatment. *Frontiers in Immunology*, *13*. https://doi.org/10.3389/fimmu.2022.813951

Trist, B. G., Hare, D. J., & Double, K. L. (2019). Oxidative stress in the aging substantia nigra and the etiology of Parkinson's disease. *Aging Cell*, *18*(6). https://doi.org/10.1111/acel.13031

Varesi, A., Chirumbolo, S., Campagnoli, L. I. M., Pierella, E., Piccini, G. B., Carrara, A., Ricevuti, G., Scassellati, C., Bonvicini, C., & Pascale, A. (2022). The Role of Antioxidants in the Interplay between Oxidative Stress and Senescence. *Antioxidants*, *11*(7), 1224. https://doi.org/10.3390/antiox11071224

Wagner, K.-D., Safwan-Zaiter, H., & Wagner, N. (2024). A Dual Role of the Senescence Marker p16Ink4a in Liver Endothelial Cell Function. *Cells*, *13*(23), 1929. https://doi.org/10.3390/cells13231929

Wang. (2010). Selective neuronal vulnerability to oxidative stress in the brain. *Frontiers in Aging Neuroscience*. https://doi.org/10.3389/fnagi.2010.00012

Wang, D.-R., & Pan, J. (2023). Extracellular vesicles: Emerged as a promising strategy for regenerative medicine. *World Journal of Stem Cells*, *15*(4), 165–181. https://doi.org/10.4252/wjsc.v15.i4.165

Wang, H., Du, Y., Xu, W., Li, C., Sun, H., Hu, K., Hu, Y., Yu, T., Guo, H., Xie, L., Wang, G., & Liang, Y. (2022). Exogenous glutathione exerts a therapeutic effect in ischemic

stroke rats by interacting with intrastriatal dopamine. *Acta Pharmacologica Sinica*, *43*(3), 541–551. https://doi.org/10.1038/s41401-021-00650-3

Wang, K., Du, Y., Li, P., Guan, C., Zhou, M., Wu, L., Liu, Z., & Huang, Z. (2024). Nanoplastics causes heart aging/myocardial cell senescence through the Ca2+/mtDNA/cGAS-STING signaling cascade. *Journal of Nanobiotechnology*, *22*(1), 96. https://doi.org/10.1186/s12951-024-02375-x

Wang, S., Qu, X., & Zhao, R. C. (2012). Clinical applications of mesenchymal stem cells. *Journal of Hematology & Oncology*, *5*(1), 19. https://doi.org/10.1186/1756-8722-5-19

Wang, Y., Fang, J., Liu, B., Shao, C., & Shi, Y. (2022). Reciprocal regulation of mesenchymal stem cells and immune responses. *Cell Stem Cell*, *29*(11), 1515–1530. https://doi.org/10.1016/j.stem.2022.10.001

Xie, H., Hu, L., & Li, G. (2010). SH-SY5Y human neuroblastoma cell line: in vitro cell model of dopaminergic neurons in Parkinson's disease. *Chinese Medical Journal*, *123*(8), 1086–1092.

Xiong, L., Pan, J.-X., Guo, H., Mei, L., & Xiong, W.-C. (2021). Parkinson's in the bone. *Cell & Bioscience*, *11*(1), 190. https://doi.org/10.1186/s13578-021-00702-5

Zagare A, Gobin M, Monzel AS, Schwamborn JC. A robust protocol for the generation of human midbrain organoids. STAR Protoc. 2021 May 4;2(2):100524. doi: 10.1016/j.xpro.2021.100524. PMID: 34027482; PMCID: PMC8121770.

Zhang, H., & Forman, H. J. (2012). Glutathione synthesis and its role in redox signaling. *Seminars in Cell & Developmental Biology*, *23*(7), 722–728. https://doi.org/10.1016/j.semcdb.2012.03.017

Zhang, L., Pitcher, L. E., Yousefzadeh, M. J., Niedernhofer, L. J., Robbins, P. D., & Zhu, Y. (2022). Cellular senescence: a key therapeutic target in aging and diseases. *Journal of Clinical Investigation*, *132*(15). https://doi.org/10.1172/JCI158450

Zhu, J., Lian, J., Wang, X., Wang, R., Pang, X., Xu, B., Wang, X., Li, C., Ji, S., & Lu, H. (2023a). Role of endogenous and exogenous antioxidants in risk of six cancers: evidence from the Mendelian randomization study. *Frontiers in Pharmacology*, *14*. https://doi.org/10.3389/fphar.2023.1185850

Zhu, J., Lian, J., Wang, X., Wang, R., Pang, X., Xu, B., Wang, X., Li, C., Ji, S., & Lu, H. (2023b). Role of endogenous and exogenous antioxidants in risk of six cancers: evidence from the Mendelian randomization study. *Frontiers in Pharmacology*, *14*. https://doi.org/10.3389/fphar.2023.1185850